

1 **Identification of two bZIP transcription factors that regulate development of**  
2 **pavement and trichome cells in *Arabidopsis thaliana* by single-cell**  
3 **RNA-sequencing**

4

5 Rui Wu<sup>1†</sup>, Zhixin Liu<sup>1†</sup>, Jiajing Wang<sup>1†</sup>, Weiqiang Li<sup>1†</sup>, Aizhi Qin<sup>1†</sup>, Xiaole Yu<sup>1†</sup>, Hao  
6 Liu<sup>1</sup>, Chenxi Guo<sup>1</sup>, Zihao Zhao<sup>1</sup>, Yixin Zhang<sup>1</sup>, Yaping Zhou<sup>1</sup>, Susu Sun<sup>1</sup>, Yumeng  
7 Liu<sup>1</sup>, Mengke Hu<sup>1</sup>, Jincheng Yang<sup>1</sup>, Masood Jan<sup>1</sup>, George Bawa<sup>1</sup>, Jean-David  
8 Rochaix<sup>2</sup>, Guoyong An<sup>1</sup>, Luis Herrera-Estrella<sup>3\*</sup>, Lam-Son Phan Tran<sup>3\*</sup>, Xuwu Sun<sup>1\*</sup>

9 1 State Key Laboratory of Crop Stress Adaptation and Improvement, State Key  
10 Laboratory of Cotton Biology, Key Laboratory of Plant Stress Biology, School of Life  
11 Sciences, Henan University, 85 Minglun Street, Kaifeng 475001, China

12 2 Departments of Molecular Biology and Plant Biology, University of Geneva,  
13 Geneva, 1211, Switzerland

14 3 Institute of Genomics for Crop Abiotic Stress Tolerance, Department of Plant and  
15 Soil Science, Texas Tech University, Lubbock, TX 79409, USA

16

17 **Running title:** bZIPs mediate trichome formation

18

19 † These authors have contributed equally to this work.

20 \*Correspondence:

21 Contact: Dr. Xuwu Sun (sunxuwu@henu.edu.cn); Dr. Lam-Son Phan Tran  
22 (son.tran@ttu.edu); Dr. Luis Herrera-Estrella (Luis.Herrera-Estrella@ttu.edu).

23 The author responsible for distribution of materials integral to the findings presented  
24 in this article in accordance with the policy described in the Instructions for Authors  
25 (<https://academic.oup.com/plcell>) is Xuwu Sun (sunxuwu@henu.edu.cn).

26

27

28 **Abstract**

29 Epidermal cells are the main avenue for signal and material exchange between plants  
30 and the environment. Leaf epidermal cells primarily include pavement cells (PCs),  
31 guard cells, and trichomes cells (TCs), which differentiate from protodermal cells or  
32 meristemoids. The development and distribution of different epidermal cells are  
33 tightly regulated by a complex transcriptional regulatory network mediated by  
34 phytohormones, including jasmonic acid (JA), and transcription factors.  
35 Understanding how the fate of leaf epidermal cells is determined, however, is still  
36 largely unknown due to the diversity of cell types and the complexity of its regulation.  
37 Here, we characterized the transcriptional profiles of epidermal cells in 3-day-old true  
38 leaves of *Arabidopsis thaliana* using single-cell RNA-sequencing. We identified two  
39 genes encoding BASIC LEUCINE-ZIPPER (bZIP) transcription factors, namely the  
40 *bZIP25* and *bZIP53*, which are highly expressed in PCs and early-stage meristemoid  
41 cells. Densities of PCs and TCs were found to increase and decrease, respectively, in  
42 *bzip25* and *bzip53* mutants, compared with wild-type plants. This trend was more  
43 pronounced in the presence of JA, suggesting that these transcription factors regulate  
44 the development of TCs and PCs in response to JA.

45

46

47

48

49

50

51

52

53

54

55

56 **IN A NUTSHELL**

57 **Background:** Leaf epidermal cells, comprised of trichome cells (TCs), guard cells  
58 (GCs), and pavement cells (PCs), are responsible for exchanging materials and  
59 information between plants and the surrounding aerial environment. Many genes have  
60 been identified in *Arabidopsis thaliana* and confirmed to be involved in the initiation  
61 and differentiation of TCs and PCs. The fate determination of TCs and PCs is tightly  
62 regulated by positive and negative regulators at the cellular level. The precise  
63 underlying molecular mechanisms responsible for the fate determination of TCs and  
64 PCs, however, are still unclear at this time.

65 **Question:** What are the transcriptomic profiles of different leaf epidermal cell types?  
66 Can we dissect the genes that are specifically expressed in certain epidermal cell types?  
67 What kinds of transcription factors are involved in regulating the fate determination of  
68 TCs and PCs?

69 **Findings:** We performed single cell RNA-seq to investigate the transcriptomic  
70 profiles of different leaf epidermal cell types and identified differentially expressed  
71 genes in each cell type. We found that genes that are involved in jasmonic acid  
72 signaling are highly expressed in early-stage meristemoid (EM) cells which can act as  
73 the precursor of PCs and perhaps of TCs. To investigate the regulatory mechanisms  
74 underlying EM development, we identified the transcription factors (TFs) in EM cells  
75 and found that two bZIP TF genes, *bZIP25* and *bZIP53*, are highly expressed in EMs.  
76 Further analyses of these two genes using both loss-of-function and gain-of-function  
77 approaches indicated that *bZIP25* and *bZIP53* are functionally involved in promoting  
78 trichome formation but inhibit pavement cell development in response to jasmonic  
79 acid.

80 **Next steps:** Besides of *bZIP25* and *bZIP53*, we also identified other key genes, for  
81 example *FES1B*, in leaf epidermal cells. Our next step will be to explore the  
82 regulation of other key genes involved in the fate determination of different cell types  
83 in leaf epidermis.



85 **Introduction**

86

87 Epidermal cells are responsible for exchanging materials and information between the  
88 plants and the surrounding aerial environment (Pathuri et al., 2008). In leaves,  
89 epidermal cells can differentiate and produce trichomes, which are a specialized cell  
90 type that protect plants from adverse conditions including ultraviolet radiation and  
91 herbivore attack (Hauser, 2014). Thus, leaf epidermal cells are comprised of trichome  
92 cells (TCs), guard cells (GCs), and pavement cells (PCs) (Marks, 1997). Previous  
93 studies have systematically and comprehensively characterized the developmental  
94 dynamics of the transcriptomes of stomatal lineage cells (Liu et al., 2020). It is now  
95 important to examine the processes underlying the fates and development of PCs and  
96 TCs.

97 Growth and development of PCs in *Arabidopsis thaliana* mainly proceed through  
98 three stages. First, initial cells with different shapes begin to expand outward along  
99 the long axis of leaves to form outward elongated polygons. Then, the cells expand  
100 laterally along the edge of the adjacent cells, and subsequently extend irregularly to  
101 the side of the adjacent cells. Finally, the cells extend further outward, and the  
102 zigzagged protrusions are staggered with the narrow indentation of adjacent cells  
103 resulting in the formation of PC with different shapes (Fu et al., 2005). The irregular  
104 zigzagged protrusions of leaf epidermis are mainly regulated by the cytoskeleton (Xu  
105 et al., 2010). The dynamic arrangement of microtubules plays a role in the  
106 development of PCs (Eng et al., 2021). Microtubule-associated proteins KATANIN,  
107 IQ67 DOMAIN5 (IQD5), SPIRAL2 and CLASP are essential for morphogenesis of  
108 PCs (Ambrose et al., 2007; Lin et al., 2013; Wightman et al., 2013; Liang et al., 2018).  
109 Microfilaments mainly control the outward projection of the edge of epidermal cells  
110 (Armour et al., 2015). The Rho GTPase cascade signaling pathway is a foundation of  
111 the formation of PCs by activating microtubules and promoting their orderly  
112 arrangement which consequently leads to morphological changes of leaf epidermal  
113 cells (Lin et al., 2013).

114        TCs are cells that originate on the epidermis of aerial organs and serve as an  
115        excellent model for the study of differentiation in plants at the cellular level (Marks,  
116        1997). TCs are regularly spaced and rarely appear adjacent to each other, suggesting  
117        that TC spacing is a tightly regulated process (Lloyd et al., 1994; Larkin et al., 1996;  
118        Schnittger et al., 1999; Esch et al., 2004; Zhao et al., 2008; Hilscher et al., 2009;  
119        Balkunde et al., 2010; Pesch and Hulskamp, 2011; Grebe, 2012; Yanagisawa et al.,  
120        2015). More than 40 genes involved in the initiation and differentiation of TCs have  
121        been identified in *Arabidopsis* (*Arabidopsis thaliana*) (Hulskamp et al., 1994; Marks  
122        et al., 2009). For example, mutations in several transcription factor (TF)-encoding  
123        genes like *GLABROUS1* (*GL1*), *GLABRA2* (*GL2*), *TRANSPARENT TESTA GLABRA1*  
124        (*TTG1*), or both *GLABRA3* (*GL3*) and *ENHANCER OF GLABRA3* (*EGL3*) result in  
125        the loss of TCs (Koornneef, 1981; Herman and Marks, 1989; Marks and Feldmann,  
126        1989; Oppenheimer et al., 1991; Hulskamp et al., 1994; Larkin et al., 1994; Rerie et  
127        al., 1994; Szymanski et al., 1998; Payne et al., 1999; Walker et al., 1999; Payne et al.,  
128        2000; Esch et al., 2003; Zhang et al., 2003; Kirik et al., 2005). Notably, both positive  
129        and negative activity of regulatory TFs are required for the development of TCs  
130        (Ishida et al., 2008; Pesch and Hulskamp, 2009). Positive regulators in *Arabidopsis*  
131        include members of several TF families, such as MYB, basic helix-loop-helix  
132        (bHLH), WDR, and C2H2 zinc finger families. R2R3-MYB TFs include *GL1* and its  
133        paralog *MYB23* (Herman and Marks, 1989; Marks and Feldmann, 1989; Kirik et al.,  
134        2001; Kirik et al., 2005; Ishida et al., 2008; Marks et al., 2009). *GL1* and *MYB23*  
135        have been reported to be functionally equivalent during TC initiation but not during  
136        the TC branching process (Kirik et al., 2005). The bHLH family members include  
137        *GL3* and its homolog *EGL3* that are involved in TC development in a partially  
138        redundant manner (Payne et al., 2000; Morohashi et al., 2007; Hao et al., 2019). TC  
139        development is activated by *TTG1*, a protein containing a WD40 repeat, a highly  
140        conserved motif consisting of approximately 40–43 amino acids, often ending with  
141        Trp-Asp (W-D) residues (Walker et al., 1999; Zhang et al., 2003). Both *GL1* and  
142        *TTG1* control the same process in TC development (Herman and Marks, 1989; Marks  
143        and Feldmann, 1989; Oppenheimer et al., 1991; Larkin et al., 1994; Walker et al.,  
144        1999; Payne et al., 2000; Kirik et al., 2005). Negative regulators of TC development  
145        include at least seven MYB proteins: *CAPRICE* (*CPC*), *TRIPTYCHON* (*TRY*),  
146        *ENHANCER OF TRY AND CPC1* (*ETC1*), *ETC2*, *ETC3*, *TRICHOMELESS1*

147 (TCL1), and TCL2 (Wada et al., 1997; Kirik et al., 2004; Kirik et al., 2004; Zhu et al.,  
148 2009; Gan et al., 2011; Tian et al., 2017). These negative regulators exhibit partially  
149 redundant roles in the initiation and differentiation of TCs. This fact is evidenced, for  
150 example, by functional studies of three genes: *CPC*, *ETC2*, and *ETC3*, in which the  
151 *cpc etc2 etc3* triple mutant exhibited an increased density of TCs compared with the  
152 single mutants (Wada et al., 1997; Kirik et al., 2004; Wang et al., 2008; Hilscher et al.,  
153 2009; Wester et al., 2009; Zhu et al., 2009). Interestingly, one study found that *ETC3*  
154 is highly expressed in young stomatal cells, and that its expression is under the control  
155 of SPEECHLESS (SPCH) which is highly expressed in early-stage meristemoid (EM)  
156 cells (Adrian et al., 2015). These results suggest that SPCH may activate genes that  
157 promote trichome differentiation, and that EM cells may act as the precursor cells for  
158 TC production.

159 Several other TFs, phytohormones, and cell developmental factors can also affect  
160 TC development (Walker et al., 2000; Breuer et al., 2009; Yoshida et al., 2009; Wen et  
161 al., 2018; Vadde et al., 2019). The TF AtMYC1 was identified as a direct target of  
162 both GL1 and GL3 in *Arabidopsis* (Pesch et al., 2013). Furthermore, a TEOSINTE  
163 BRANCHED1, CYCLOIDIA, and PROLIFERATING CELL NUCLEAR ANTIGEN  
164 FACTOR1/2 (TCP) TF family member, namely TCP4, was reported to affect TC fate  
165 by directly binding to the promoters of *TCL1* and *TCL2*, which in turn repress *GL2*  
166 (Efroni et al., 2008). The positive regulators of TC initiation GL1 and GL2 are  
167 significantly up-regulated in *TCP4* loss-of-function mutants and down-regulated in  
168 gain-of-function mutants (Vadde et al., 2019). Previous studies have also indicated  
169 that wounding and jasmonate (JA) significantly promote TC initiation (Traw and  
170 Bergelson, 2003; Li et al., 2004; Boughton et al., 2005; Qi et al., 2011; Tian et al.,  
171 2016; Yan et al., 2017). Qi et al., (2011) found that JA ZIM-domain (JAZ) repressor  
172 proteins interact with bHLH (Transparent Testa8, GL3, and EGL3) and R2R3-MYB  
173 TFs (e.g., MYB75 and GLABRA1), which are the essential components of  
174 WD-repeat/bHLH/MYB transcriptional complexes (Qi et al., 2011). JAZ proteins are  
175 substrates of the CORONATINE INSENSITIVE1 (COI1)-based SCF<sup>COI1</sup> E3 ligase  
176 complex (Gupta et al., 2021). Upon JA binding with COI1, COI1 recruits JAZ  
177 proteins to the SCF<sup>COI1</sup> E3 complex for ubiquitination and degradation through the  
178 26S proteasome (Chini et al., 2007). Subsequently, the bHLH and MYB components  
179 of WD-repeat/bHLH/MYB complexes are released and the development of TCs is

180 activated (Qi et al., 2011). Regarding the TC development, two proteins, SIAMESE  
181 (SIM) and STICHEL (STI), play a fundamental role in the regulation of the  
182 endoreduplication of nuclear DNA (Walker et al., 2000; Ilgenfritz et al., 2003;  
183 Churchman et al., 2006).

184 Several transcriptomic studies of TC development have been conducted to  
185 explore the regulatory processes responsible for the development of TCs and to  
186 identify new regulatory factors associated with TC development (Marks et al., 2008;  
187 Marks et al., 2009; Wang et al., 2009; Chen et al., 2014; Yang et al., 2015; Akhtar et  
188 al., 2017). These initial studies have characterized the transcriptome of TCs and  
189 identified several marker genes associated with the regulation of TC development and  
190 function. Transcriptome analysis of TCs alone, however, cannot dissect the regulation  
191 of the fate determination of TCs at the gene expression level. This is because the fate  
192 determination of TCs is also affected by fate determination factors and the  
193 developmental status of PCs that are adjacent to TCs, which can potentially  
194 differentiate into TCs (Grebe, 2012). The fate determination of TCs and PCs is tightly  
195 regulated by positive and negative regulators at the cellular level. The precise  
196 underlying molecular mechanisms responsible for the fate determination of TCs and  
197 PCs, however, are still unclear. Single-cell RNA-sequencing (scRNA-seq) technology  
198 allows the analysis of transcriptional profiles of different types of cells and to identify  
199 genes that are specifically expressed at different developmental and morphogenetic  
200 stages (Zhang et al., 2019; Liu et al., 2020; Wendrich et al., 2020; Kim et al., 2021;  
201 Liu et al., 2021; Serrano-Ron et al., 2021; Liu et al., 2022). Therefore, we conducted a  
202 scRNA-seq analysis of 3-day-old true leaves of *Arabidopsis* wild-type (WT) to  
203 elucidate the mechanisms that regulate the fate and development of TCs and PCs. Our  
204 study identified a group of novel marker genes for PCs and TCs, and discovered the  
205 new roles of two BASIC LEUCINE-ZIPPER (bZIP) TFs in the regulation of fate  
206 determination and differentiation of PCs and TCs through the comparative analysis of  
207 WT and single and double mutants of *bZIP25* and *bZIP53* genes.

208

## 209 **Results**

210

### 211 **Single-cell transcriptional profiles of leaf epidermal cells unravels different cell 212 types and gene expression signatures**

213 We subjected protoplasts of 3-day-old true leaves of *Arabidopsis* to scRNA-seq  
214 analysis to identify cell type-specific changes in gene expression that occur during  
215 epidermal cell fate determination at a single-cell resolution (Figure 1A-D). Protoplasts  
216 were filtered through a 40  $\mu$ m cell strainer and cell viability was assessed by phenol  
217 blue staining. A total of 18,000 cells were subsequently used to generate the libraries  
218 that were sequenced (Figure 1B and C). After stringent cell filtration, high-quality  
219 transcriptomes of 15,773 individual cells were retained for subsequent analyses  
220 (Figure 1D). A total of 512,130,798 reads were obtained after processing the  
221 sequencing data, with an average of 32,468 reads and 2,118 genes identified per cell.  
222 The percentage of reads mapped to the genome was 93%. We then performed  
223 t-distributed stochastic neighbor embedding (tSNE) dimensionality analysis of the  
224 scRNA-seq data. Supplemental Figure S1A and B illustrate the tSNE projection plots  
225 of cells colored by unique molecular identifier (UMI) counts and automated clustering,  
226 respectively.

227 The sequencing saturation satisfied the requirement of 10 $\times$ genomics  
228 (Supplemental Figure S1C). The median number of genes per cell (using TAIR10 as  
229 the reference genome) also met the requirement for data analysis (Supplemental  
230 Figure S1D). We then analyzed the scRNA-seq data by principal component analysis  
231 (PCA). Supplemental Figure S1E shows the distribution of the percent of  
232 mitochondrial gene sequences (percent. mito) on a PCA plot. Supplemental Figure  
233 S1F and G display the UMI distribution (nUMI) and number of nuclear-encoded  
234 genes (nGene) on the PCA plot. After removing mitochondrial and chloroplast  
235 transcripts, a total of 14,464 cells were used for the subsequent analysis  
236 (Supplemental Figure S1H). Subsequently, tSNE analysis was carried out on the  
237 selected cells. As shown in Figure 1E, 9 cell clusters were identified as being  
238 independently distributed on the tSNE plot. We also visualized cell clusters using the  
239 uniform manifold approximation and projection (UMAP) algorithm on our  
240 scRNA-seq data (Supplemental Figure S2). The UMAP analysis produced similar cell  
241 clusters as those in the tSNE analysis (Supplemental Figure S2A and S2B). We  
242 identified differentially expressed genes (DEGs) in the different cell types  
243 (Supplemental Table S1 and Table S2). The expression patterns of the top 10 marker  
244 genes in each cell type are shown in a heatmap plot (Figure 2A and Supplemental

245 [Figure S2C](#)). The violin plots and feature plots of representative marker genes in each  
246 cell type are shown in [Figure 2B and C](#) and [Supplemental Figure S2D](#).

247 We then determined the cell type of the identified cell clusters using well-defined  
248 cell type-specific marker genes for epidermal cells. As shown in [Figures 1F and 2A-C](#),  
249 the epidermal marker gene for PCs, *TCP21*, was chiefly expressed in cluster 0; the  
250 marker gene for mesophyll cells (MPCs), *RIBULOSE BISPHOSPHATE*  
251 *CARBOXYLASE LARGE CHAIN (RBCL)*, was primarily distributed in cluster 1; the  
252 marker gene for EMs, *UDP-DEPENDENT GLYCOSYLTRANSFERASE 76B1*  
253 (*UGT76B1*), was mainly expressed in cluster 2; the marker gene for GCs,  
254 *BETA-GLUCOSIDASE (BGLU30)*, was predominantly distributed in cluster 3; the  
255 late-stage meristemoid cells (LMs) marker genes, *DNA BINDING WITH ONE*  
256 *FINGER 4.6 (DOF4.6)* and *bZIP9*, were mainly enriched in cluster 5; the meristemoid  
257 mother cell (MMC) marker gene, *HOMEODOMAIN GLABROUS 2 (HDG2)*, was  
258 chiefly expressed in cluster 6; the young guard cells (YGCs) marker gene, *HIGH*  
259 *CARBON DIOXIDE (HIC)*, was mainly expressed in cluster 7; the guard mother cell  
260 (GMC) marker genes, *FAMA* and *DOF5.7*, were mostly expressed in cluster 8.  
261 However, the marker gene for TCs, *GL2* (Szymanski et al., 1998), was unfortunately  
262 not detected in our scRNA-seq data, perhaps because the size of TCs was too large to  
263 pass through the cell strainer. Thus, no known marker genes were identified to be  
264 expressed in cluster 4. Collectively, our results indicate that cluster 0 belongs to PCs;  
265 cluster 1 belongs to MPCs; cluster 2 belongs to EMs; cluster 3 belongs to GCs; cluster  
266 4 belongs to unknown (u.k.) cells; cluster 5 belongs to LMs; cluster 6 belongs to  
267 MMCs; cluster 7 belongs to YGCs; cluster 8 belongs to GMCs. Notably, the  
268 expression of some marker genes of the JA signal transduction pathway, such as  
269 *ACYL-COA OXIDASE 1 (ACXI)* (Peng et al., 2019), *ABNORMAL INFLORESCENCE*  
270 *MERISTEM (AIM1)* (Delker et al., 2007), *BLADE ON PETIOLE1 (BOP1)* (Canet et  
271 al., 2012), *CORONATINE INSENSITIVE 1 (COII)* (Xie et al., 1998; Thines et al.,  
272 2007), *CONSTITUTIVE EXPRESSION OF PR GENES 5 (CPR5)* (Clarke et al., 2001),  
273 *CULLIN 1 (CUL1)* (Quint et al., 2005); *JASMONATE-ZIM-DOMAIN PROTEIN 10*  
274 (*JAZ10*) (Chung and Howe, 2009), *JASMONATE-INDUCED OXYGENASE2 (JAO2)*,  
275 *JASMONATE-INDUCED OXYGENASE3 (JAO3)* (Caarls et al., 2017),  
276 *PRODUCTION OF ANTHOCYANIN PIGMENT 1 (PAPI)* (Bali et al., 2019),  
277 *RADICAL-INDUCED CELL DEATH1 (RCD1)* (Overmyer et al., 2000), and

278 *RIBONUCLEASE 1 (RNS1)* (LeBrasseur et al., 2002) was also significant in cluster 2,  
279 suggesting that they may function in EMs ([Supplemental Figure S3](#)).

280

281 **Selection and characterization of newly identified marker genes in PCs and EMs**

282 Gene ontology (GO) analysis was then performed to identify the potential biological  
283 function of DEGs in each cell cluster ([Supplemental Table S3](#)). As shown in  
284 [Supplemental Figure S4](#), GO terms in MPCs and PCs were generally very similar and  
285 different from the other cell types. GO terms in the u.k., LM, GMC, and EM clusters  
286 were comparable, suggesting that these genes are involved in similar biological  
287 processes in these different cell types. GO terms for MPCs were predominantly  
288 related to photosynthesis, consistent with the functions of MPCs ([Supplemental](#)  
289 [Figure S4](#)). Considering the high similarity in GO terms in clusters 3 and 7, we  
290 propose that cluster 3 belongs to GCs ([Supplemental Figure S4](#)). We could not  
291 identify TCs by the expression of the TC marker gene *GL2* because the size of TCs  
292 was too large to pass through the cell strainer. In our previous study, we found that  
293 some marker genes were detected in several cell types but at different levels of  
294 expression (Liu et al., 2020). The top 10 marker genes for each of the studied cell  
295 types other than TCs were specifically expressed in the corresponding cell types,  
296 except for the markers of MPCs, GMCs, and GCs. Some marker genes of PCs, such  
297 as *FERREDOXIN C 2 (FDC2)*, *FES1B*, *AT2G29290*, and *EPIDERMAL*  
298 *PATTERNING FACTOR LIKE-9 (EPFL9)*, were also enriched in MPCs and GCs  
299 ([Figure 2A](#)).

300 Transgenic plants expressing yellow fluorescent protein (YFP) fusion proteins of  
301 some of the representative genes were generated to determine the cellular localization  
302 of the proteins encoded by the selected marker genes. The expression of YFP was  
303 detected in PCs for TCP21, FDC2, NADH DEHYDROGENASE-LIKE COMPLEX  
304 M (NDHM), AT1G70820, AT2G29290, and AT5G02590 ([Supplemental Figure S5](#)).  
305 YFP signals for FDC2 and NDHM were also detected in GCs. The localization of  
306 AT5G02590 and PECTIN METHYLESTERASE 17 (PME17) in PCs and EMs could  
307 not be distinguished from each other. YFP signals for bZIP9 were detected in GCs,  
308 although its expression was mostly in LMs ([Figure 2A](#) and [Supplemental Figure S5](#)).  
309 In general, the expression patterns of the selected genes were consistent with the  
310 results presented in [Figure 2A](#). We also constructed promoter-driven *GUS* reporter

311 gene vectors for some of the representative genes to analyze the tissue specificity of  
312 gene expression. *AT2G29290*, *FES1B*, *TCP21*, *PLASTID TRANSCRIPTIONALLY*  
313 *ACTIVE 18* (*PTAC18*), *FDC2*, and *AT1G64355* were selected as marker genes for PCs,  
314 while *AT1G04950* and *EUKARYOTIC RELEASE FACTOR 1-2* (*ERF1-2*) were  
315 selected as marker genes for EMs, and the corresponding transgenic plants were  
316 produced. GUS staining analysis revealed that the selected genes are expressed in the  
317 leaves of seedlings (Figure 3). Some genes, such as *TCP21*, *FDC2*, *ERF1-2*, and  
318 *AT1G04950*, can also expressed in roots (Figure 3), suggesting these genes may also  
319 play an important function in root epidermal cells.

320 Transgenic plants were also successfully produced that overexpressed several  
321 selected newly identified PC (e.g., *TCP21*, *AT1G70820*, *AT2G29290*, *FDC2*, *FES1B*,  
322 *NDHM*, *EPFL9*, and *PTAC18*) and EM (e.g., *AT5G02590*, *AT3G48020*, *AT4G18422*,  
323 *AT3G10530*, and *AT4G23620*) marker genes to determine their potential roles in the  
324 regulation of PC and TC development. Results indicated that, compared with WT  
325 plants, overexpression of *TCP21*, *FDC2*, *AT4G18422*, and *AT4G23620* resulted in a  
326 significant decrease in the density of TCs, while overexpression of *FES1B*, *NDHM*,  
327 and *AT3G10530* enhanced the density of TCs (Figure 4A and C). PC density was  
328 significantly lower, relative to WT plants, in seedlings of *35S::FES1B*, *35S::PTAC18*,  
329 *35S::FDC2*, and *35S::AT3G48020* transgenic plants, but significantly higher in  
330 *35S::EPFL9* and *35S::AT4G23620* transgenic seedlings (Figure 4B and D). Leaf area  
331 in *35S::TCP21* plants was also significantly smaller than in WT plants (Figure 4E).  
332 These results suggest that the selected PC and EM marker genes may be involved in  
333 the development of PCs and TCs.

334

335 **Pseudo-time trajectory analysis of the spatiotemporal dynamics of epidermal cell**  
336 **differentiation**

337 Arabidopsis leaf development is a strictly regulated process that ensures that almost  
338 all leaves have similar spatial morphological characteristics at the same  
339 developmental stage (Byrne et al., 2001; Fleming, 2005; Bar and Ori, 2014). The  
340 spatiotemporal regulation of leaf development is closely related to that of cell  
341 development (Kalve et al., 2014; Lu et al., 2014). Therefore, understanding the  
342 spatiotemporal regulation pattern of cell development is important for understanding

343 leaf development. Taking this into consideration, we performed a pseudo-temporal  
344 ordering of cells (pseudo-time) on the scRNA-seq data using Monocle 2 (Trapnell et  
345 al., 2014) to reconstruct the developmental trajectory during differentiation. The  
346 resulting pseudo-time path has two nodes and three branches (Figure 5A), and  
347 different cell clusters are arranged relatively clearly at different branch sites of the  
348 pseudo-time path (Figure 5B). A heatmap analysis based on pseudo-time results was  
349 then constructed to characterize the spatiotemporal dynamic patterns of the top 10  
350 genes of each cluster. As shown in Figure 5C, the heatmap of several representative  
351 genes from each cluster indicated a positive correlation between their expression  
352 dynamics and their cell distribution on the developmental trajectory. For example,  
353 *UGT76B1* and *PEROXIDASE 71 (PER71)* are maximally expressed in the pre-branch  
354 of the pseudo-time trajectory, while *TPC21* and *EPFL9* are mostly expressed in the  
355 late stage of cell fate 1 (Figure 5C). Marker genes of stomatal lineage cells, such as  
356 *HIC* and *DOF5.7*, have their highest expression levels in the early stage of cell  
357 development, while these genes are down-regulated following the developmental  
358 direction of cell fate 1 and cell fate 2 (Figure 5C). These results indicate that genes  
359 expressed in different cell types have a specific spatiotemporal pattern on the  
360 pseudo-time trajectory.

361

### 362 **Analysis of the effects of JA on the development of TCs and PCs**

363 Since JA signaling marker genes are expressed in EMs (Supplemental Figure S3), it is  
364 possible that JA could be involved in the regulation of EM differentiation. It has been  
365 proposed that EMs give rise to both PCs and TCs (Adrian et al., 2015), and JA plays  
366 important roles in regulating the development of TCs (Yan et al., 2017). Therefore, to  
367 explore this possibility, we first analyzed the process of TC differentiation in WT  
368 seedlings in the presence of JA. Results indicated that the number of TCs significantly  
369 increased in the presence of 20  $\mu$ M JA (Supplemental Figure S6). Higher  
370 concentrations of JA ( $> 40 \mu$ M) inhibit leaf growth, although the density of TCs  
371 gradually increases with the increasing JA dose (Supplemental Figure S6B and C).  
372 We then analyzed the effects of JA on the development of PCs, and found that the

373 density of PCs decreased along with the increasing JA concentrations (0 to 40  $\mu$ M)  
374 ([Supplemental Figure S7](#)).

375

### 376 **bZIP TFs are involved in regulating the fate of PCs and TCs**

377 TFs play important roles in regulating the development of all kinds of cells. For  
378 example, SPCH, FAMA, MUTE, and BASIC PENTACYSTEINE 6 (BPC6) TFs are  
379 essential for the development of GCs (Liu et al., 2020). In our search for potential  
380 regulators of PCs and TCs, we identified two TF-encoding genes, *bZIP25* and *bZIP53*,  
381 that were predominantly expressed in EMs and PCs ([Figure 6A and B](#)), raising the  
382 possibility that they may be involved in regulating the fate and differentiation of these  
383 cells. GUS expression can be detected in the true leaves of *bZIP25pro::GUS*  
384 transgenic plants ([Supplemental Figure S8A](#)). Notably, YFP signals in *bZIP25*-YFP  
385 plants were highly detected in the nuclei of PCs ([Supplemental Figure S8B](#)). We then  
386 examined the corresponding T-DNA insertion mutants *bzip25* and *bzip53* obtained  
387 from the Arabidopsis Biological Resource Center (ABRC) to investigate the potential  
388 roles of *bZIP25* and *bZIP53* in the regulation of PC and TC development. The  
389 developmental states of TCs in leaves of the single mutant *bzip25* and *bzip53*  
390 seedlings are shown in [Figure 6C](#). Results indicated that TC densities in *bzip25* and  
391 *bzip53* seedlings were lower than in WT plants with and without JA treatment, but the  
392 response to JA was decreased in the mutants as compared with the WT ([Figure 6E](#)). In  
393 contrast, the analysis of PCs showed that PC density in *bzip25* and *bzip53* mutant  
394 seedlings was higher than in the WT with and without JA-treatment ([Figure 6F](#)).  
395 Consistently, a greater number of TCs was observed in *35S::bZIP25* and *35S::bZIP53*  
396 plants, while the number of PCs in *35S::bZIP25* and *35S::bZIP53* plants was lower  
397 than the WT ([Figure 6C—F](#)). These results indicate that *bZIP25* and *bZIP53* play a  
398 positive role in determining the density of TCs and a negative role in the density of  
399 PCs

400 Next, to test whether *bZIP25* and *bZIP53* function in the same regulatory  
401 pathway of epidermal cell development, we generated the double mutants *bzip25*  
402 *bzip53-1* and *bzip25 bzip53-2* using CRISPR/Cas9 technology ([Figure 6C](#) and  
403 [Supplemental Figure S9](#)). Under control conditions (no JA), the number of TCs was  
404 lower in the double mutants, relative to the single mutants and WT plants, while the  
405 number of PCs was greater ([Figure 6D and F](#)). The effects of JA on TC and PC

406 development were weak in the double mutants, relative to the single mutants and WT  
407 plants (Figure 6A–D). These results collectively suggest that *bZIP25* and *bZIP53*  
408 might play additive or partially redundant roles in regulating the fate and  
409 differentiation of PCs and TCs (Figure 7).

410

## 411 Discussion

412

### 413 Identification of marker genes in cell clusters obtained by scRNA-seq of young 414 leaves

415 Utilizing scRNA-seq technology, we constructed the global landscape of the  
416 transcriptomes of young epidermal cell types in leaves. Unlike cotyledons, leaf  
417 epidermal cell types are more complex with the most striking feature being the  
418 development of TCs. The fate determination and differentiation of TCs are tightly  
419 regulated by both internal factors, such as hormones, and external cues, such as  
420 invading pests and pathogens (Ishida et al., 2008). The transcriptome of TCs has been  
421 extensively characterized but not at the single-cell level (Marks et al., 2008; Marks et  
422 al., 2009). Also, for true leaves, no reported studies on epidermal cells at single-cell  
423 resolution are available. TCs are differentiated from protodermal cells or EMs (Adrian  
424 et al., 2015). Therefore, a comprehensive study of the transcriptomes of different  
425 epidermal cell types in true leaves will enable us to identify the potential key  
426 regulators of the differentiation and development of different cell types in the leaf  
427 epidermis. Because EMs, PCs and TCs of true leaves have certain interaction in  
428 differentiation and development (Adrian et al., 2015), we can identify the regulatory  
429 factors regulating TCs by analyzing the key regulatory factors in EMs and PCs. In the  
430 scRNA-seq data obtained in this study, we did not identify the cell type in which the  
431 well-known TC marker gene *GL2* is specifically expressed (Figure 1). One possible  
432 explanation is that the size of TCs is too large and filtered out during the process of  
433 cell filtration used to prepare protoplast for scRNA-seq. Therefore, in this work we  
434 mainly focused on the characterization of the transcriptomes of EMs and PCs. We  
435 identified several genes that specifically expressed in EMs and PCs (Figure 2 and

436 [Supplemental Figure S2](#)). To verify the cell types identified in the present study, we  
437 generated *GUS* reporter constructs for representative marker genes in PCs and EMs  
438 ([Figure 3](#)). Analysis of the expression pattern of the *GUS* reporter constructs indicated  
439 that the marker genes for PCs (including *AT2G29290*, *FES1B*, *TCP21*, *PTAC18*, and  
440 *FDC2*) and EMs (including *AT1G04950*, *AT4G18422*, *bZIP25*, and *ERF1-2*) are  
441 highly expressed in true leaves ([Figure 3](#)). Since EM cells and PCs are distributed  
442 among the entire upper epidermal layer of true leaves, *GUS* expression, which was  
443 controlled by the promoter of the marker genes expressed in EMs and PCs, appears to  
444 occur in all epidermal cells ([Figure 3](#)). We also generated transgenic plants expressing  
445 YFP fusion proteins of some of the representative marker genes to detect their cell  
446 expression pattern. As predicted, the expression of PC marker genes, such as  
447 *AT2G29290*, *FDC2*, *NDHM*, *AT1G70820*, and *TCP21*, were detected in PCs  
448 ([Supplemental Figure S5](#)). The expression of the EM marker genes, *AT5G02590* and  
449 *PME17*, however, was also observed in PCs ([Supplemental Figure S5](#)), which is  
450 consistent with the fact that PCs develop from EM cells (Adrian et al., 2015) ([Figure  
451 1G](#)). In our study, *bZIP9* expression was detected in GCs ([Supplemental Figure S5](#)),  
452 however, a recent study has reported that *bZIP9* is strongly expressed in phloem  
453 parenchyma cells (Kim et al., 2021). *NDHM* and *FDC2* were also found to express in  
454 GCs ([Supplemental Figure S5](#)). The specific expression of the examined marker genes  
455 in PCs and EM cells suggests that these genes may be involved in mediating the  
456 development of these two cell types ([Figure 3](#)). Analysis of the developmental status  
457 of TCs and PCs in seedlings of transgenic plants overexpressing selected newly  
458 identified marker genes revealed that *TCP21*, *FDC2*, *AT5G02590*, *AT4G18422*, and  
459 *AT4G23620* negatively affect TC development, while *FES1B*, *NDHM*, and *EPFL9*  
460 positively affect TC development ([Figure 4](#)). Our results also demonstrated that  
461 *FES1B* negatively regulates the development of PCs, while *EPFL9* and *AT4G23620*  
462 regulate PC development in a positive manner ([Figure 4](#)). At present, the distinction  
463 between PCs and EM cells is difficult due to the inability to define specific marker

464 genes. Our results provide important data that can be used for identifying PCs and EM  
465 cells in future scRNA-seq studies of epidermal cell development.

466

467 **Dissection of the spatiotemporal patterns of the transcriptomes of epidermal cells  
468 in true leaves**

469 GCs, PCs, EM cells, and TCs are the main cell types present in the upper epidermis of  
470 leaves of *A. thaliana*. PCs, EM cells, and GCs differentiate from MMCs. According to  
471 the distribution of cells in the constructed pseudo-time trajectories, MMCs mainly  
472 appear at the initial stage, while EM cells and GCs are distributed over the later stages  
473 of pseudo-time trajectories (Figure 5B). This is consistent with the viewpoint that  
474 GCs and EMs differentiate from MMCs (Liu et al., 2020). Formation of TCs was  
475 highly similar to that of EMs in regard to developmental regulation (Adrian et al.,  
476 2015). Therefore, the results of the pseudo-time trajectory of EMs also support the  
477 evidence indicating that EMs or TCs are differentiated from MMCs. Pseudo-time  
478 heatmap analysis of the top 10 genes further confirmed this premise (Figure 5C). Our  
479 results indicate that the analysis of the spatiotemporal patterns of gene expression in  
480 specific types of cells significantly contributes to the understanding of their  
481 development.

482

483 **bZIP TFs are involved in regulating the fate and development of EMs and TCs  
484 in response to JA signaling**

485 Identification of key TFs in specific cell types can assist in the identification of  
486 important regulatory factors involved in the fate determination and development of  
487 specific cell types. *bZIP25* and *bZIP53* were identified in our analysis of TF-encoding  
488 genes with increased expression in PCs and EMs (Figure 6A and B). Previous studies  
489 have shown that JA promotes the development of TCs (Yan et al., 2017), but inhibits  
490 the development of leaves (Noir et al., 2013). Our results demonstrated that high  
491 concentrations of JA inhibited leaf growth, but that TCs density gradually increased  
492 as the applied dose of JA increased (Supplemental Figure S6B and C). Further  
493 analysis of the effects of JA on the developmental status of both PCs and TCs in  
494 seedlings of the *bzip25* and *bzip53* single and double mutants revealed that *bZIP25*

495 and *bZIP53* may have additive or partially redundant functions in the regulation of  
496 development of PCs and TCs (Figure 7). In summary, our results provide new insights  
497 into the mechanisms underlying the highly complex yet orderly orchestrated process  
498 of epidermal cell development. These findings provide a basis for the further study of  
499 novel regulators of specific cell types in the epidermis of leaves.

500

## 501 **Materials and methods**

502

### 503 **Screening and verification of mutants**

504 Wild-type (WT) and *A. thaliana* (Col-0 ecotype) were used in the scRNA-seq  
505 experiments. Seeds were sterilized in 5% sodium hypochlorite and germinated on  
506 vertical, half-strength Murashige and Skoog (1/2 MS) plates. T-DNA insertion  
507 mutants were obtained from the Arabidopsis Biological Resource Center (ABRC)  
508 (Supplemental Table 4). Mutant lines homozygous for the T-DNA insertion were  
509 identified by PCR analysis using gene-specific and T-DNA-specific primers  
510 (Supplemental Table 5 and Supplemental Figure S10). All mutants and WT plants  
511 were grown in a climate chamber at 22°C and 100  $\mu\text{mol}$  photons  $\text{m}^{-2} \text{ s}^{-1}$  under a 14-h  
512 light/10-h dark regime. In the experiments designed to examine the effect of JA on the  
513 TC development, 3-day-old seedlings were treated by spraying methyl jasmonate  
514 (392707, Millipore Sigma, St Louis, MO, USA). The seedlings were then placed in a  
515 sealed transparent plastic container that allowed them to continue to grow for a  
516 defined period of time. The developmental status of TCs was photographically  
517 documented.

518

### 519 **Constructs for plant transformation**

520 *YFP-fusion expression constructs* - full-length cDNA fragments of marker genes were  
521 PCR-amplified using the primer pairs described in Supplemental Table 5. The  
522 resulting PCR products were purified and cloned into pDNOR201 by BP Clonase  
523 reactions (GATEWAY Cloning; Invitrogen, Waltham, MA, USA) according to the  
524 manufacturer's instructions to generate the pDONR-cDNA vectors. The resulting  
525 plasmids were then recombined into pB7YWG2.0 using LR Clonase reactions to  
526 generate the final constructs.

527 *GUS reporter constructs* - the upstream 2,000-bp fragments of marker genes were

528 PCR-amplified using the primer pairs described in [Supplemental Table 5](#). The  
529 resulting PCR products were purified and cloned into pDNOR201 by BP Clonase  
530 reactions according to the manufacturer's instructions to generate the pDONR-cDNA  
531 vectors. The resulting plasmids were recombined into pBGWFS7 using LR Clonase  
532 reactions to generate the final constructs. The resulting reporter constructs were then  
533 used to detect the expression of GUS under the control of the promoters of the  
534 different marker genes.

535

### 536 **Plant transformation**

537 YFP-fusion expression constructs and reporter constructs were transformed into  
538 *Agrobacterium tumefaciens* strain GV3101 via electroporation. *A. tumefaciens*  
539 containing the different constructs were introduced into WT plants. The resulting T1  
540 transgenic plants containing YFP-fusion expression constructs and reporter constructs  
541 were selected using BASTA as described previously (Sun et al., 2016). Homozygous  
542 transgenic plants were used in all experiments.

543

### 544 **Sample collection and protoplast preparation**

545 Three-day-old true leaves were harvested and used to isolate protoplasts as previously  
546 described with slight modifications to adjust for the use of young leaf tissues (Yoo et  
547 al., 2007; Liu et al., 2020).

548

### 549 **ScRNA-seq library preparation**

550 ScRNA-seq libraries were prepared using a Chromium Single Cell 3' Gel  
551 Beads-in-emulsion (GEM) Library & Gel Bead Kit v3 according to the  
552 manufacturer's instructions (10 $\times$  Genomics, California, USA).

553

### 554 **ScRNA-seq data preprocessing**

555 The raw data were processed as previously described (Liu et al., 2020). After the  
556 critical filtering process, 14,464 out of 15,773 cells were retained for downstream  
557 analysis. The median value of the mapping rate was 66.8%, and the median number of  
558 genes detected in each cell was 2,118. Library size normalization was performed in  
559 Seurat on the filtered matrix to obtain normalized counts.

560

561 **Clustering analysis of scRNA-seq data**

562 Genes with the greatest variable expression amongst single cells were identified using  
563 the method described by (Macosko et al., 2015). The tSNE analysis, UMAP analysis,  
564 and DEG identification were performed as previously described (Liu et al., 2020; Liu  
565 et al., 2022).

566

567 **Pseudo-time and trajectory analysis**

568 Pseudo-time trajectory analysis of single-cell transcriptomes was conducted using  
569 Monocle 2 (Trapnell et al., 2014) as previously described (Liu et al., 2020).

570

571 **Bulk and scRNA-seq correlation analysis**

572 Bulk and scRNA-seq correlation analysis was performed as described (Rheaume et al.,  
573 2018). Differential expression was analyzed with a *t*-test. The *t*-test function was used  
574 to test the gene expression value in scRNA-seq and bulk, and a significant *P*-value  
575 was obtained. The difference multiple of  $\log_2$  (FC) was calculated as follows:  $\log_2$   
576  $([\text{mean gene expression value in scRNA-seq}] + 0.001) / ([\text{mean gene expression value}]$   
577  $+ 0.001)$ . Finally, genes with a significant difference in expression were  
578 identified based on a *p*-value  $< 0.05$  and  $|\log_2(\text{FC})| > 1$ .

579

580 **RNA-seq analysis**

581 Three-day-old true leaves were harvested for extraction of total RNA using a mirVana  
582 miRNA Isolation Kit (Ambion, Waltham, MA, USA) following the manufacturer's  
583 protocol. Samples with an RNA Integrity Number (RIN)  $\geq 7$  were subjected to  
584 subsequent RNA-seq analysis. Libraries were constructed using a TruSeq Stranded  
585 mRNA LT Sample Prep Kit (Illumina, San Diego, CA, USA) according to the  
586 manufacturer's instructions. Libraries were sequenced on an Illumina sequencing  
587 platform (HiSeqTM 2500 or Illumina HiSeq X Ten), and 125-bp/150-bp paired-end  
588 reads were generated.

589

590 **GUS staining and histological analysis**

591 Histochemical GUS staining was performed with a G3061 GUS staining Kit (Solarbio  
592 Co., Beijing, China) according to the manufacturer's instructions as previously  
593 described (Liu et al., 2022).

594

595 **Microscopy**

596 Seedlings were stained with 10 g mL<sup>-1</sup> propidium iodide (PI) (P4170, Sigma, St Louis,  
597 MO, USA) for 1 min prior to imaging. PI staining was used to stain the cell wall of  
598 epidermal cells. Fluorescence in roots was detected using a Zeiss LSM980 confocal  
599 laser scanning microscope (Zeiss, Oberkochen, Germany). The PI signal was  
600 visualized at 610 to 630 nm wavelengths. YFP was observed at 510 to 530 nm  
601 wavelengths. Images and GFP intensities were processed using Zeiss Confocal  
602 Software.

603

604 **GO enrichment analysis**

605 GO enrichment pathway analyses for the DEGs were conducted in Metascape  
606 (<http://metascape.org/>) (Zhou et al., 2019).

607

608 **Accession numbers**

609 The accession numbers for some of the selected genes are as follows: *AT5G08330*  
610 (*TCP21*), *AT3G53800* (*FES1B*), *AT3G54620* (*bZIP25*), *AT3G58750* (*CSY2*),  
611 *AT3G62420* (*bZIP53*), *AT1G32550* (*FDC2*), *AT3G11340* (*UGT76B1*), *AT2G28110*  
612 (*FRA8/IRX7*), *AT4G12970* (*STOMAGEN/EPFL9*), *AT1G12920* (*ERF1-2*),  
613 *AT2G42790* (*CSY3*), *AT4G37925* (*NDHM*), *AT2G32180* (*PTAC18*), *AT1G69480*  
614 (*PHO1-H10*), *AT1G70820*, *AT5G16030*, *AT2G29290*, *AT1G64355*, *AT5G02590*,  
615 *AT3G48020*, *AT4G18422*, *AT3G10530*, *AT2G35480*, *AT4G23620* and *AT1G04945*.  
616 ScRNA-seq data are available at the following web addresses:  
617 (<https://dataview.ncbi.nlm.nih.gov/?search=SUB6947465>;  
618 <https://www.ncbi.nlm.nih.gov>).

619

620 **Supplemental data**

621 The following materials are available in the online version of this article.

622 **Supplemental Figure S1.** Analysis of the single-cell RNA-sequencing (scRNA-seq)  
623 raw data.

624 **Supplemental Figure S2.** Comparative analysis of the cell clusters identified with  
625 different methods of dimensionality reduction.

626 **Supplemental Figure S3.** The expression pattern of jasmonic acid (JA) marker  
627 genes.

628 **Supplemental Figure S4.** GO and KEGG analysis of the differentially expressed  
629 genes (DEGs) in each of the cell clusters.

630 **Supplemental Figure S5.** Analysis of the expression of marker genes.

631 **Supplemental Figure S6.** Jasmonic acid (JA) promotes the development of TCs.

632 **Supplemental Figure S7.** Jasmonic acid (JA) inhibits the development of PCs.

633 **Supplemental Figure S8.** Analysis of the expression of bZIP25.

634 **Supplemental Figure S9.** Analysis of the DNA sequence in *bzip25* and *bzip53*  
635 seedlings after DNA editing.

636 **Supplemental Figure S10.** Verification of the T-DNA insertion in mutants.

637 **Supplemental Table 1.** All\_DEGs\_for\_all\_clusters\_tSNE.

638 **Supplemental Table 2.** All\_DEGs\_for\_all\_clusters\_UMAP.

639 **Supplemental Table 3.** GO analysis of differentially expressed genes (DEGs).

640 **Supplemental Table 4.** List of mutant lines used in the study.

641 **Supplemental Table 5.** List of oligonucleotide primer pairs used in the study.

642

643 **Acknowledgments**

644 We are grateful to ABRC for the *Arabidopsis* seeds. This research was supported by  
645 the National Natural Science Foundation of China (31670233).

646

647 **Author contributions**

648 Conceptualization of the project: X.S. Experimental design: X.S and Z.L. Performance  
649 of some specific experiments: R.W., Z.L. J.W., A.Q., X.Y., H.L., Z.Z., Yixin Zhang,  
650 C.G., Yaping Zhou, M.J., G.B., S.S., Y.L., M.H., and J.Y. Data analysis: W.L., J.W.,  
651 Y.Z., G.A. and J.R. Manuscript drafting: S.X. Contribution to the editing and  
652 proofreading of the manuscript draft: J.R., L.E., and L.T. All authors have read and  
653 approved the final manuscript.

654 *Conflict of interest statement.* Authors declare no conflict of interest.

655

656 **Data Availability Statement**

657 All data supporting the findings of this study are available within the paper and the

658 supplementary data published online.

659

660 **References**

661

662 **Adrian J, Chang J, Ballenger CE, Bargmann BO, Alassimone J, Davies KA, Lau OS, Matos JL, Hachez C, Lanctot A, Vaten A, Birnbaum KD, Bergmann DC** (2015) Transcriptome dynamics of the stomatal lineage: birth, amplification, and termination of a self-renewing population. *Dev Cell* **33**: 107-118

663 **Akhtar MQ, Qamar N, Yadav P, Kulkarni P, Kumar A, Shasany AK** (2017) Comparative glandular trichome transcriptome-based gene characterization reveals reasons for differential (-)-menthol biosynthesis in *Mentha* species. *Physiol Plant* **160**: 128-141

664 **Ambrose JC, Shoji T, Kotzer AM, Pighin JA, Wasteneys GO** (2007) The *Arabidopsis* CLASP gene encodes a microtubule-associated protein involved in cell expansion and division. *Plant Cell* **19**: 2763-2775

665 **Armour WJ, Barton DA, Law AM, Overall RL** (2015) Differential Growth in Periclinal and Anticlinal Walls during Lobe Formation in *Arabidopsis* Cotyledon Pavement Cells. *Plant Cell* **27**: 2484-2500

666 **Bali S, Jamwal VL, Kohli SK, Kaur P, Tejpal R, Bhalla V, Ohri P, Gandhi SG, Bhardwaj R, Al-Huqail AA, Siddiqui MH, Ali HM, Ahmad P** (2019) Jasmonic acid application triggers detoxification of lead (Pb) toxicity in tomato through the modifications of secondary metabolites and gene expression. *Chemosphere* **235**: 734-748

667 **Balkunde R, Pesch M, Hulskamp M** (2010) Trichome patterning in *Arabidopsis thaliana* from genetic to molecular models. *Curr Top Dev Biol* **91**: 299-321

668 **Bar M, Ori N** (2014) Leaf development and morphogenesis. *Development* **141**: 4219-4230

669 **Boughton AJ, Hoover K, Felton GW** (2005) Methyl jasmonate application induces increased densities of glandular trichomes on tomato, *Lycopersicon esculentum*. *J Chem Ecol* **31**: 2211-2216

670 **Breuer C, Kawamura A, Ichikawa T, Tominaga-Wada R, Wada T, Kondou Y, Muto S, Matsui M, Sugimoto K** (2009) The trihelix transcription factor GTL1 regulates ploidy-dependent cell growth in the *Arabidopsis* trichome. *Plant Cell* **21**: 2307-2322

671 **Byrne M, Timmermans M, Kidner C, Martienssen R** (2001) Development of leaf shape. *Curr Opin Plant Biol* **4**: 38-43

672 **Caarls L, Elberse J, Awwanah M, Ludwig NR, de Vries M, Zeilmaker T, Van Wees SCM, Schuurink RC, Van den Ackerveken G** (2017) *Arabidopsis* JASMONATE-INDUCED OXYGENASES down-regulate plant immunity by hydroxylation and inactivation of the hormone jasmonic acid. *Proc Natl Acad Sci U S A* **114**: 6388-6393

673 **Canet JV, Dobon A, Fajmonova J, Tornero P** (2012) The BLADE-ON-PETIOLE genes of *Arabidopsis* are essential for resistance induced by methyl jasmonate. *BMC Plant Biol* **12**: 199

697 **Chen C, Liu M, Jiang L, Liu X, Zhao J, Yan S, Yang S, Ren H, Liu R, Zhang X** (2014)  
698 Transcriptome profiling reveals roles of meristem regulators and polarity genes during fruit  
699 trichome development in cucumber (*Cucumis sativus* L.). *J Exp Bot* **65**: 4943-4958

700 **Chini A, Fonseca S, Fernandez G, Adie B, Chico JM, Lorenzo O, Garcia-Casado G, Lopez-Vidriero I, Lozano FM, Ponce MR, Micol JL, Solano R** (2007) The JAZ family of  
701 repressors is the missing link in jasmonate signalling. *Nature* **448**: 666-+

702 **Chung HS, Howe GA** (2009) A critical role for the TIFY motif in repression of jasmonate signaling by  
703 a stabilized splice variant of the JASMONATE ZIM-domain protein JAZ10 in *Arabidopsis*.  
704 *Plant Cell* **21**: 131-145

705 **Churchman ML, Brown ML, Kato N, Kirik V, Hulskamp M, Inze D, De Veylder L, Walker JD, Zheng Z, Oppenheimer DG, Gwin T, Churchman J, Larkin JC** (2006) SIAMESE, a  
706 plant-specific cell cycle regulator, controls endoreplication onset in *Arabidopsis thaliana*. *Plant  
Cell* **18**: 3145-3157

707 **Clarke JD, Aarts N, Feys BJ, Dong X, Parker JE** (2001) Constitutive disease resistance requires  
708 EDS1 in the *Arabidopsis* mutants cpr1 and cpr6 and is partially EDS1-dependent in cpr5.  
709 *Plant J* **26**: 409-420

710 **Delker C, Zolman BK, Miersch O, Wasternack C** (2007) Jasmonate biosynthesis in *Arabidopsis  
thaliana* requires peroxisomal beta-oxidation enzymes--additional proof by properties of pex6  
711 and aim1. *Phytochemistry* **68**: 1642-1650

712 **Efroni I, Blum E, Goldshmidt A, Eshed Y** (2008) A protracted and dynamic maturation schedule  
713 underlies *Arabidopsis* leaf development. *Plant Cell* **20**: 2293-2306

714 **Eng RC, Schneider R, Matz TW, Carter R, Ehrhardt DW, Jonsson H, Nikoloski Z, Sampathkumar A** (2021) KATANIN and CLASP function at different spatial scales to  
715 mediate microtubule response to mechanical stress in *Arabidopsis* cotyledons. *Curr Biol* **31**:  
716 3262-+

717 **Esch JJ, Chen M, Sanders M, Hillestad M, Ndkium S, Idelkope B, Neizer J, Marks MD** (2003) A  
718 contradictory GLABRA3 allele helps define gene interactions controlling trichome  
719 development in *Arabidopsis*. *Development* **130**: 5885-5894

720 **Esch JJ, Chen MA, Hillestad M, Marks MD** (2004) Comparison of TRY and the closely related  
721 At1g01380 gene in controlling *Arabidopsis* trichome patterning. *Plant J* **40**: 860-869

722 **Fleming AJ** (2005) The control of leaf development. *New Phytol* **166**: 9-20

723 **Fu Y, Gu Y, Zheng Z, Wasteneys G, Yang Z** (2005) *Arabidopsis* interdigitating cell growth requires  
724 two antagonistic pathways with opposing action on cell morphogenesis. *Cell* **120**: 687-700

725 **Gan L, Xia K, Chen JG, Wang S** (2011) Functional characterization of TRICHOMELESS2, a new  
726 single-repeat R3 MYB transcription factor in the regulation of trichome patterning in  
727 *Arabidopsis*. *BMC Plant Biol* **11**: 176

728 **Grebe M** (2012) The patterning of epidermal hairs in *Arabidopsis*--updated. *Curr Opin Plant Biol* **15**:  
729 31-37

730 **Gupta A, Bhardwaj M, Tran LP** (2021) JASMONATE ZIM-DOMAIN Family Proteins: Important  
731 Nodes in Jasmonic Acid-Abscisic Acid Crosstalk for Regulating Plant Response to Drought.  
732 *Curr Protein Pept Sci* **22**: 759-766

733

734

735

736

737

738 **Hao J, Cao W, Huang J, Zou X, Han ZG** (2019) Optimal Gene Filtering for Single-Cell data  
739 (OGFSC)-a gene filtering algorithm for single-cell RNA-seq data. *Bioinformatics* **35**:  
740 2602-2609

741 **Hauser MT** (2014) Molecular basis of natural variation and environmental control of trichome  
742 patterning. *Front Plant Sci* **5**: 320

743 **Herman PL, Marks MD** (1989) Trichome Development in *Arabidopsis thaliana*. II. Isolation and  
744 Complementation of the GLABROUS1 Gene. *Plant Cell* **1**: 1051-1055

745 **Hilscher J, Schlotterer C, Hauser MT** (2009) A single amino acid replacement in ETC2 shapes  
746 trichome patterning in natural *Arabidopsis* populations. *Curr Biol* **19**: 1747-1751

747 **Hulskamp M, Misra S, Jurgens G** (1994) Genetic dissection of trichome cell development in  
748 *Arabidopsis*. *Cell* **76**: 555-566

749 **Ilgenfritz H, Bouyer D, Schnittger A, Mathur J, Kirik V, Schwab B, Chua NH, Jurgens G, Hulskamp M** (2003) The *Arabidopsis* STICHEL gene is a regulator of trichome branch  
750 number and encodes a novel protein. *Plant Physiol* **131**: 643-655

751 **Ishida T, Kurata T, Okada K, Wada T** (2008) A genetic regulatory network in the development of  
752 trichomes and root hairs. *Annu Rev Plant Biol* **59**: 365-386

753 **Kalve S, De Vos D, Beemster GT** (2014) Leaf development: a cellular perspective. *Front Plant Sci* **5**:  
754 362

755 **Kim JY, Symeonidi E, Pang TY, Denyer T, Weidauer D, Bezrutczyk M, Miras M, Zollner N, Hartwig T, Wudick MM, Lercher M, Chen LQ, Timmermans MCP, Frommer WB** (2021)  
756 Distinct identities of leaf phloem cells revealed by single cell transcriptomics. *Plant Cell* **33**:  
757 511-530

758 **Kirik V, Lee MM, Wester K, Herrmann U, Zheng Z, Oppenheimer D, Schiefelbein J, Hulskamp M** (2005) Functional diversification of MYB23 and GL1 genes in trichome morphogenesis  
759 and initiation. *Development* **132**: 1477-1485

760 **Kirik V, Schnittger A, Radchuk V, Adler K, Hulskamp M, Baumlein H** (2001) Ectopic expression  
761 of the *Arabidopsis* AtMYB23 gene induces differentiation of trichome cells. *Dev Biol* **235**:  
762 366-377

763 **Kirik V, Simon M, Hulskamp M, Schiefelbein J** (2004) The ENHANCER OF TRY AND CPC1  
764 gene acts redundantly with TRIPTYCHON and CAPRICE in trichome and root hair cell  
765 patterning in *Arabidopsis*. *Dev Biol* **268**: 506-513

766 **Kirik V, Simon M, Wester K, Schiefelbein J, Hulskamp M** (2004) ENHANCER of TRY and CPC 2  
767 (ETC2) reveals redundancy in the region-specific control of trichome development of  
768 *Arabidopsis*. *Plant Mol Biol* **55**: 389-398

769 **Koornneef M** (1981) The complex syndrome of TTG mutants. *arabid.inf.serv*

770 **Larkin JC, Oppenheimer DG, Lloyd AM, Paparozzi ET, Marks MD** (1994) Roles of the  
771 GLABROUS1 and TRANSPARENT TESTA GLABRA Genes in *Arabidopsis* Trichome  
772 Development. *Plant Cell* **6**: 1065-1076

773 **Larkin JC, Oppenheimer DG, Marks MD** (1994) The GL1 gene and the trichome developmental  
774 pathway in *Arabidopsis thaliana*. *Results Probl Cell Differ* **20**: 259-275

775 **Larkin JC, Young N, Prigge M, Marks MD** (1996) The control of trichome spacing and number in  
776 *Arabidopsis*. *Development* **122**: 997-1005

780 **LeBrasseur ND, MacIntosh GC, Perez-Amador MA, Saitoh M, Green PJ** (2002) Local and  
781 systemic wound-induction of RNase and nuclease activities in *Arabidopsis*: RNS1 as a marker  
782 for a JA-independent systemic signaling pathway. *Plant J* **29**: 393-403

783 **Li L, Zhao Y, McCaig BC, Wingerd BA, Wang J, Whalon ME, Pichersky E, Howe GA** (2004) The  
784 tomato homolog of CORONATINE-INSENSITIVE1 is required for the maternal control of  
785 seed maturation, jasmonate-signaled defense responses, and glandular trichome development.  
786 *Plant Cell* **16**: 126-143

787 **Liang H, Zhang Y, Martinez P, Rasmussen CG, Xu T, Yang Z** (2018) The Microtubule-Associated  
788 Protein IQ67 DOMAIN5 Modulates Microtubule Dynamics and Pavement Cell Shape. *Plant*  
789 *Physiol* **177**: 1555-1568

790 **Lin D, Cao L, Zhou Z, Zhu L, Ehrhardt D, Yang Z, Fu Y** (2013) Rho GTPase signaling activates  
791 microtubule severing to promote microtubule ordering in *Arabidopsis*. *Curr Biol* **23**: 290-297

792 **Liu Q, Liang Z, Feng D, Jiang SJ, Wang YF, Du ZY, Li RX, Hu GH, Zhang PX, Ma YF,  
793 Lohmann JU, Gu XF** (2021) Transcriptional landscape of rice roots at the single-cell  
794 resolution. *Mol Plant* **14**: 384-394

795 **Liu Z, Wang J, Zhou Y, Zhang Y, Qin A, Yu X, Zhao Z, Wu R, Guo C, Bawa G, Rochaix JD, Sun  
796 X** (2022) Identification of Novel Regulators Required for Early Development of Vein Pattern  
797 in the Cotyledons by Single-cell RNA-seq. *Plant J*

798 **Liu Z, Zhou Y, Guo J, Li J, Tian Z, Zhu Z, Wang J, Wu R, Zhang B, Hu Y, Sun Y, Shangguan Y,  
799 Li W, Li T, Hu Y, Guo C, Rochaix JD, Miao Y, Sun X** (2020) Global Dynamic Molecular  
800 Profiles of Stomatal Lineage Cell Development by Single-Cell RNA Sequencing. *Mol Plant*

801 **Lloyd AM, Schena M, Walbot V, Davis RW** (1994) Epidermal cell fate determination in *Arabidopsis*:  
802 patterns defined by a steroid-inducible regulator. *Science* **266**: 436-439

803 **Lu D, Wang T, Persson S, Mueller-Roeber B, Schippers JH** (2014) Transcriptional control of ROS  
804 homeostasis by KUODA1 regulates cell expansion during leaf development. *Nat Commun* **5**:  
805 3767

806 **Macosko EZ, Basu A, Satija R, Nemesh J, Shekhar K, Goldman M, Tirosh I, Bialas AR,  
807 Kamitaki N, Martersteck EM, Trombetta JJ, Weitz DA, Sanes JR, Shalek AK, Regev A,  
808 McCarroll SA** (2015) Highly Parallel Genome-wide Expression Profiling of Individual Cells  
809 Using Nanoliter Droplets. *Cell* **161**: 1202-1214

810 **Marks MD** (1997) Molecular Genetic Analysis of Trichome Development in *Arabidopsis*. *Annu Rev  
811 Plant Physiol Plant Mol Biol* **48**: 137-163

812 **Marks MD, Betancur L, Gilding E, Chen F, Bauer S, Wenger JP, Dixon RA, Haigler CH** (2008) A  
813 new method for isolating large quantities of *Arabidopsis* trichomes for transcriptome, cell wall  
814 and other types of analyses. *Plant J* **56**: 483-492

815 **Marks MD, Feldmann KA** (1989) Trichome Development in *Arabidopsis thaliana*. I. T-DNA Tagging  
816 of the GLABROUS1 Gene. *Plant Cell* **1**: 1043-1050

817 **Marks MD, Wenger JP, Gilding E, Jilk R, Dixon RA** (2009) Transcriptome analysis of *Arabidopsis*  
818 wild-type and gl3-sst sim trichomes identifies four additional genes required for trichome  
819 development. *Mol Plant* **2**: 803-822

820 **Morohashi K, Zhao M, Yang M, Read B, Lloyd A, Lamb R, Grotewold E** (2007) Participation of  
821 the *Arabidopsis* bHLH factor GL3 in trichome initiation regulatory events. *Plant Physiol* **145**:  
822 736-746

823 **Noir S, Bomer M, Takahashi N, Ishida T, Tsui TL, Balbi V, Shanahan H, Sugimoto K, Devoto A**  
824 (2013) Jasmonate Controls Leaf Growth by Repressing Cell Proliferation and the Onset of  
825 Endoreduplication while Maintaining a Potential Stand-By Mode. *Plant Physiol* **161**:  
826 1930-1951

827 **Oppenheimer DG, Herman PL, Sivakumaran S, Esch J, Marks MD** (1991) A myb gene required  
828 for leaf trichome differentiation in *Arabidopsis* is expressed in stipules. *Cell* **67**: 483-493

829 **Overmyer K, Tuominen H, Kettunen R, Betz C, Langebartels C, Sandermann H, Jr., Kangasjarvi**  
830 **J** (2000) Ozone-sensitive *arabidopsis rcd1* mutant reveals opposite roles for ethylene and  
831 jasmonate signaling pathways in regulating superoxide-dependent cell death. *Plant Cell* **12**:  
832 1849-1862

833 **Pathuri IP, Zellerhoff N, Schaffrath U, Hensel G, Kumlehn J, Kogel KH, Eichmann R,**  
834 **Huckelhoven R** (2008) Constitutively activated barley ROPs modulate epidermal cell size,  
835 defense reactions and interactions with fungal leaf pathogens. *Plant Cell Rep* **27**: 1877-1887

836 **Payne CT, Zhang F, Lloyd AM** (2000) GL3 encodes a bHLH protein that regulates trichome  
837 development in *arabidopsis* through interaction with GL1 and TTG1. *Genetics* **156**:  
838 1349-1362

839 **Payne T, Clement J, Arnold D, Lloyd A** (1999) Heterologous myb genes distinct from GL1 enhance  
840 trichome production when overexpressed in *Nicotiana tabacum*. *Development* **126**: 671-682

841 **Peng S, Huang S, Liu Z, Feng H** (2019) Mutation of ACX1, a Jasmonic Acid Biosynthetic Enzyme,  
842 Leads to Petal Degeneration in Chinese Cabbage (*Brassica campestris* ssp. *pekinensis*). *Int J*  
843 *Mol Sci* **20**

844 **Pesch M, Hulskamp M** (2009) One, two, three...models for trichome patterning in *Arabidopsis*? *Curr*  
845 *Opin Plant Biol* **12**: 587-592

846 **Pesch M, Hulskamp M** (2011) Role of TRIPTYCHON in trichome patterning in *Arabidopsis*. *BMC*  
847 *Plant Biol* **11**: 130

848 **Pesch M, Schultheiss I, Digiuni S, Uhrig JF, Hulskamp M** (2013) Mutual control of intracellular  
849 localisation of the patterning proteins AtMYC1, GL1 and TRY/CPC in *Arabidopsis*.  
850 *Development* **140**: 3456-3467

851 **Qi T, Song S, Ren Q, Wu D, Huang H, Chen Y, Fan M, Peng W, Ren C, Xie D** (2011) The  
852 Jasmonate-ZIM-domain proteins interact with the WD-Repeat/bHLH/MYB complexes to  
853 regulate Jasmonate-mediated anthocyanin accumulation and trichome initiation in *Arabidopsis*  
854 *thaliana*. *Plant Cell* **23**: 1795-1814

855 **Quint M, Ito H, Zhang W, Gray WM** (2005) Characterization of a novel temperature-sensitive allele  
856 of the CUL1/AXR6 subunit of SCF ubiquitin-ligases. *Plant J* **43**: 371-383

857 **Rerie WG, Feldmann KA, Marks MD** (1994) The GLABRA2 gene encodes a homeo domain protein  
858 required for normal trichome development in *Arabidopsis*. *Genes Dev* **8**: 1388-1399

859 **Rheaume BA, Jereen A, Bolisetty M, Sajid MS, Yang Y, Renna K, Sun L, Robson P,**  
860 **Trakhtenberg EF** (2018) Single cell transcriptome profiling of retinal ganglion cells  
861 identifies cellular subtypes. *Nat Commun* **9**: 2759

862 **Schnittger A, Folkers U, Schwab B, Jurgens G, Hulskamp M** (1999) Generation of a spacing  
863 pattern: the role of triptychon in trichome patterning in *Arabidopsis*. *Plant Cell* **11**: 1105-1116

864 **Serrano-Ron L, Perez-Garcia P, Sanchez-Corriñero A, Gude I, Cabrera J, Ip PL, Birnbaum KD, Moreno-Risueno MA** (2021) Reconstruction of lateral root formation through single-cell RNA sequencing reveals order of tissue initiation. *Mol Plant* **14**: 1362-1378

865 **Sun XW, Xu DR, Liu ZX, Kleine T, Leister D** (2016) Functional relationship between mTERF4 and GUN1 in retrograde signaling. *J Exp Bot* **67**: 3909-3924

866 **Szymanski DB, Jilk RA, Pollock SM, Marks MD** (1998) Control of GL2 expression in Arabidopsis leaves and trichomes. *Development* **125**: 1161-1171

867 **Thines B, Katsir L, Melotto M, Niu Y, Mandaokar A, Liu G, Nomura K, He SY, Howe GA, Browse J** (2007) JAZ repressor proteins are targets of the SCF(CO11) complex during jasmonate signalling. *Nature* **448**: 661-665

868 **Tian H, Qi T, Li Y, Wang C, Ren C, Song S, Huang H** (2016) Regulation of the WD-repeat/bHLH/MYB complex by gibberellin and jasmonate. *Plant Signal Behav* **11**: e1204061

869 **Tian H, Wang X, Guo H, Cheng Y, Hou C, Chen JG, Wang S** (2017) NTL8 Regulates Trichome Formation in Arabidopsis by Directly Activating R3 MYB Genes TRY and TCL1. *Plant Physiol* **174**: 2363-2375

870 **Trapnell C, Cacchiarelli D, Grimsby J, Pokharel P, Li S, Morse M, Lennon NJ, Livak KJ, Mikkelsen TS, Rinn JL** (2014) The dynamics and regulators of cell fate decisions are revealed by pseudotemporal ordering of single cells. *Nat Biotechnol* **32**: 381-386

871 **Traw MB, Bergelson J** (2003) Interactive effects of jasmonic acid, salicylic acid, and gibberellin on induction of trichomes in Arabidopsis. *Plant Physiol* **133**: 1367-1375

872 **Vadde BVL, Challa KR, Sunkara P, Hegde AS, Nath U** (2019) The TCP4 Transcription Factor Directly Activates TRICHOMELESS1 and 2 and Suppresses Trichome Initiation. *Plant Physiol* **181**: 1587-1599

873 **Wada T, Tachibana T, Shimura Y, Okada K** (1997) Epidermal cell differentiation in Arabidopsis determined by a Myb homolog, CPC. *Science* **277**: 1113-1116

874 **Walker AR, Davison PA, Bolognesi-Winfield AC, James CM, Srinivasan N, Blundell TL, Esch JJ, Marks MD, Gray JC** (1999) The TRANSPARENT TESTA GLABRA1 locus, which regulates trichome differentiation and anthocyanin biosynthesis in Arabidopsis, encodes a WD40 repeat protein. *Plant Cell* **11**: 1337-1350

875 **Walker JD, Oppenheimer DG, Concienne J, Larkin JC** (2000) SIAMESE, a gene controlling the endoreduplication cell cycle in *Arabidopsis thaliana* trichomes. *Development* **127**: 3931-3940

876 **Wang S, Hubbard L, Chang Y, Guo J, Schiefelbein J, Chen JG** (2008) Comprehensive analysis of single-repeat R3 MYB proteins in epidermal cell patterning and their transcriptional regulation in Arabidopsis. *BMC Plant Biol* **8**: 81

877 **Wang W, Wang Y, Zhang Q, Qi Y, Guo D** (2009) Global characterization of *Artemisia annua* glandular trichome transcriptome using 454 pyrosequencing. *BMC Genomics* **10**: 465

878 **Wen J, Li Y, Qi T, Gao H, Liu B, Zhang M, Huang H, Song S** (2018) The C-terminal domains of Arabidopsis GL3/EGL3/TT8 interact with JAZ proteins and mediate dimeric interactions. *Plant Signal Behav* **13**: e1422460

879 **Wendrich JR, Yang B, Vandamme N, Verstaen K, Smet W, Van de Velde C, Minne M, Wybouw B, Mor E, Arents HE, Nolf J, Van Duyse J, Van Isterdael G, Maere S, Saeys Y, De Rybel B**

906 (2020) Vascular transcription factors guide plant epidermal responses to limiting phosphate  
907 conditions. *Science* **370**

908 **Wester K, Digiuni S, Geier F, Timmer J, Fleck C, Hulskamp M** (2009) Functional diversity of R3  
909 single-repeat genes in trichome development. *Development* **136**: 1487-1496

910 **Wightman R, Chomicki G, Kumar M, Carr P, Turner SR** (2013) SPIRAL2 determines plant  
911 microtubule organization by modulating microtubule severing. *Curr Biol* **23**: 1902-1907

912 **Xie DX, Feys BF, James S, Nieto-Rostro M, Turner JG** (1998) COI1: an *Arabidopsis* gene required  
913 for jasmonate-regulated defense and fertility. *Science* **280**: 1091-1094

914 **Xu T, Wen M, Nagawa S, Fu Y, Chen JG, Wu MJ, Perrot-Rechenmann C, Friml J, Jones AM,**  
915 **Yang Z** (2010) Cell surface- and rho GTPase-based auxin signaling controls cellular  
916 interdigitation in *Arabidopsis*. *Cell* **143**: 99-110

917 **Yan T, Chen M, Shen Q, Li L, Fu X, Pan Q, Tang Y, Shi P, Lv Z, Jiang W, Ma YN, Hao X, Sun X,**  
918 **Tang K** (2017) HOMEODOMAIN PROTEIN 1 is required for jasmonate-mediated glandular  
919 trichome initiation in *Artemisia annua*. *New Phytol* **213**: 1145-1155

920 **Yanagisawa M, Desyatova AS, Belteton SA, Mallery EL, Turner JA, Szymanski DB** (2015)  
921 Patterning mechanisms of cytoskeletal and cell wall systems during leaf trichome  
922 morphogenesis. *Nat Plants* **1**: 15014

923 **Yang C, Gao Y, Gao S, Yu G, Xiong C, Chang J, Li H, Ye Z** (2015) Transcriptome profile analysis of  
924 cell proliferation molecular processes during multicellular trichome formation induced by  
925 tomato Wo (v) gene in tobacco. *Genom Data* **6**: 173-174

926 **Yoo SD, Cho YH, Sheen J** (2007) *Arabidopsis* mesophyll protoplasts: a versatile cell system for  
927 transient gene expression analysis. *Nat Protoc* **2**: 1565-1572

928 **Yoshida Y, Sano R, Wada T, Takabayashi J, Okada K** (2009) Jasmonic acid control of GLABRA3  
929 links inducible defense and trichome patterning in *Arabidopsis*. *Development* **136**: 1039-1048

930 **Zhang F, Gonzalez A, Zhao M, Payne CT, Lloyd A** (2003) A network of redundant bHLH proteins  
931 functions in all TTG1-dependent pathways of *Arabidopsis*. *Development* **130**: 4859-4869

932 **Zhang TQ, Xu ZG, Shang GD, Wang JW** (2019) A Single-Cell RNA Sequencing Profiles the  
933 Developmental Landscape of *Arabidopsis* Root. *Mol Plant* **12**: 648-660

934 **Zhao M, Morohashi K, Hatlestad G, Grotewold E, Lloyd A** (2008) The TTG1-bHLH-MYB  
935 complex controls trichome cell fate and patterning through direct targeting of regulatory loci.  
936 *Development* **135**: 1991-1999

937 **Zhou Y, Zhou B, Pache L, Chang M, Khodabakhshi AH, Tanaseichuk O, Benner C, Chanda SK**  
938 (2019) Metascape provides a biologist-oriented resource for the analysis of systems-level  
939 datasets. *Nat Commun* **10**: 1523

940 **Zhu HF, Fitzsimmons K, Khandelwal A, Kranz RG** (2009) CPC, a single-repeat R3 MYB, is a  
941 negative regulator of anthocyanin biosynthesis in *Arabidopsis*. *Mol Plant* **2**: 790-802

942

943

944 **Figures and legends**

945

946 **Figure 1. Distinct cell subpopulations with transcriptional signatures determined**  
947 **by single-cell RNA-sequencing analysis of epidermal cells of true leaves. (A-D)**  
948 Illustration of the scheme used for young leaves (A), cell isolation (B), sequencing  
949 (C), and downstream analysis (D). E, t-distributed stochastic neighbor embedding  
950 (tSNE) plot reveals cellular heterogeneity with 9 distinct clusters of cells identified  
951 and color-coded. General identity of each cell cluster is defined in the corresponding  
952 cluster. F, Feature plots of expression distribution for selected marker genes.  
953 Expression levels for each cell are color-coded and overlaid onto the tSNE plot. G,  
954 Illustration of a leaf section with the different cell types. TC, trichome cell; EM,  
955 early-stage meristemoid; GC, guard cell; PC, pavement cell; LM, late-stage  
956 meristemoid; YCG, young guard cell; MPC, mesophyll cell; GMC, guard mother cell;  
957 MMC, meristemoid mother cell; u.k., unknown.

958

959 **Figure 2. Identification of novel marker genes for each cluster.** A, Heatmap of  
960 differentially expressed genes (DEGs). The top 5 genes and their relative expression  
961 levels in all sequenced cells are shown for each cluster. The color ranges from purple  
962 to yellow and represents the expression value of the marker genes from low to high. B,  
963 Violin plots of selected novel marker genes for each cluster. C, Feature plots of the  
964 expression distribution of selected novel marker genes. Expression levels for each cell  
965 are color-coded and superimposed on the tSNE plot. EM, early-stage meristemoid;  
966 GC, guard cell; PC, pavement cell; LM, late-stage meristemoid; YCG, young guard  
967 cell; MPC, mesophyll cell; GMC, guard mother cell; MMC, meristemoid mother cell;  
968 u.k., unknown.

969

970 **Figure 3. Expression of selected marker genes in different tissues.** Transgenic  
971 plants expressing the *GUS* reporter gene driven by the promoters of the selected  
972 marker genes were generated to analyze their expression patterns. GUS signals were  
973 detected by staining. Scale bar, 2 mm is shown as a blue line.

974

975 **Figure 4. Characterization of the potential roles of selected marker genes for**  
976 **pavement cells (PCs) and trichome cells (TCs).** A, Detection of the  
977 developmental status of trichomes in transgenic lines and wild-type (WT) seedlings.  
978 Scale bar (0.5 mm) is shown as a red line with a white background. B, Analysis of the  
979 developmental status of PCs in WT and transgenic lines. Samples were stained with  
980 propidium iodide, after which PCs were detected using a laser confocal microscope.  
981 Scale bar (50  $\mu$ m) is shown as a white line. C, TC density in the upper epidermis of  
982 two 3-day-old true leaves of WT and transgenic seedlings. D, PC density in the upper  
983 epidermis of 3-day-old true leaves of WT and transgenic seedlings. Data represent a  
984 mean  $\pm$  SD ( $n = 3$ ). Asterisks indicate a significant difference between transgenic and  
985 WT plants as determined using a Student's *t*-test. \* $P < 0.05$ , \*\* $p < 0.01$ , and \*\*\* $p <$   
986 0.001. ns, non-significant.

987

988 **Figure 5. Pseudo-time analysis reveals putative differentiation trajectories of**  
989 **different cell types.** A, Distribution of cells of each cluster on the pseudo-time  
990 trajectory. B, Distribution of cells of each cell type on the pseudo-time trajectory. C,  
991 Clustering and expression kinetics of the top 10 genes in all clusters along with a  
992 pseudo-time progression. EM, early-stage meristemoid; GC, guard cell; PC, pavement  
993 cell; LM, late-stage meristemoid; YCG, young guard cell; MPC, mesophyll cell;  
994 GMC, guard mother cell; MMC, meristemoid mother cell; u.k., unknown.

995

996 **Figure 6. bZIP25 and bZIP53 positively regulate trichome cell (TC) development**  
997 **and negatively regulate pavement cell (PC) development.** A, Violin plots showing  
998 the expression of *bZIP25* and *bZIP53* in EMs and PCs. B, Feature plots showing the  
999 expression of *bZIP25* and *bZIP53* in EMs and PCs. C, Representative photographs of  
1000 the upper epidermis of 3-day-old true leaves of WT, *bzip25*, *bzip53*, *bzip25 bzip53*,  
1001 *35S::bZIP25* and *35S::bZIP53* plants subjected to 0 (control) and 40  $\mu$ M jasmonic  
1002 acid (JA) treatments. Bar, 500  $\mu$ m. D, Representative photographs of PCs in the upper  
1003 epidermis of 3-day-old true leaves of WT, *bzip25*, *bzip53*, *bzip25 bzip53*, *35S::bZIP25*  
1004 and *35S::bZIP53* plants subjected to 0 (control) and 40  $\mu$ M jasmonic acid (JA)  
1005 treatments. The samples were treated by propidium iodide (PI) staining to show the  
1006 cell wall. Bar, 50  $\mu$ m. (E-F) Density of TCs (E) and density of PCs (F) in the upper

1007 epidermis of two 3-day-old true leaves of WT, *bzip25*, *bzip53*, *bzip25 bzip53*,  
1008 *35S::bZIP25* and *35S::bZIP53* plants subjected to 0 and 40  $\mu$ M JA treatments. Data  
1009 represent a mean  $\pm$  SD ( $n = 3$ ). Asterisks indicate a significant difference between  
1010 mutant and WT, and between overexpression lines and WT as determined using a  
1011 Student's *t*-test. \* $P < 0.05$ , \*\* $p < 0.01$ , and \*\*\* $p < 0.001$ . ns, non-significant. Letters  
1012 indicate a significant difference between single mutant and double mutant as  
1013 determined using a Student's *t*-test. <sup>a</sup>  $P < 0.05$ , <sup>b</sup>  $P < 0.01$ .

1014

1015 **Figure 7. Model of the transcription factor network, including bZIP25 and**  
1016 **bZIP53, in regulating TC and PC development.** The fate of a TC is regulated by a  
1017 series of critical transcription factors, including TTG1, GL2, MYC1, GL3, SIM, and  
1018 TCPs, as well as others. JA positively promotes the development of TC but inhibits  
1019 the differentiation of PC. bZIP25 and bZIP53, in response to JA, negatively regulate  
1020 the fate of a PC and may positively promote the differentiation of a TC.

1021

1022

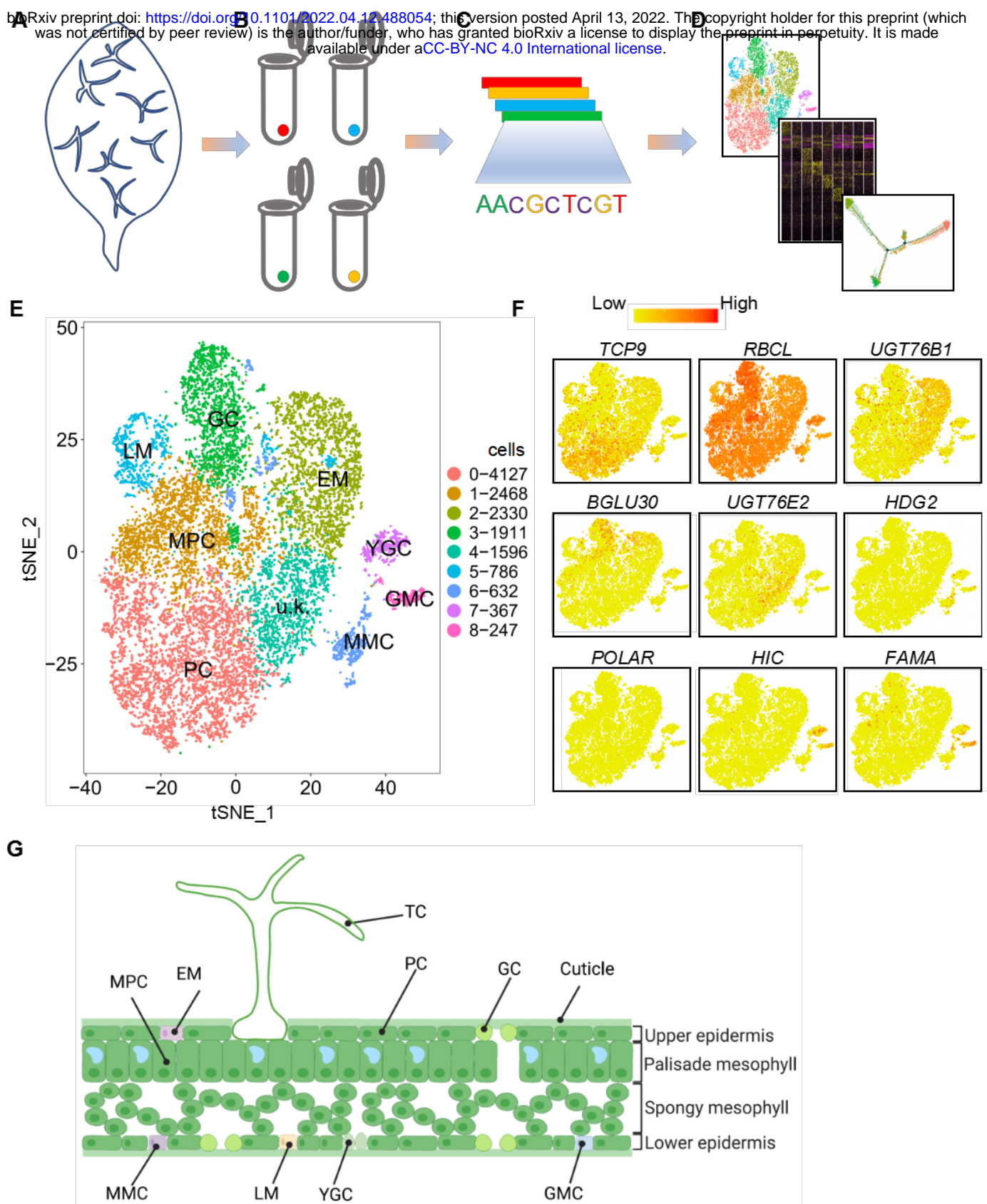


**Figure 1. Distinct cell subpopulations with transcriptional signatures determined by single-cell RNA-sequencing analysis of epidermal cells of true leaves.** (A-D) Illustration of the scheme used for young leaves (A), cell isolation (B), sequencing (C), and downstream analysis (D). E, t-distributed stochastic neighbor embedding (tSNE) plot reveals cellular heterogeneity with 9 distinct clusters of cells identified and color-coded. General identity of each cell cluster is defined in the corresponding cluster. F, Feature plots of expression distribution for selected marker genes. Expression levels for each cell are color-coded and overlaid onto the tSNE plot. G, Illustration of a leaf section with the different cell types. TC, trichome cell; EM, early-stage meristemoid; GC, guard cell; PC, pavement cell; LM, late-stage meristemoid; YCG, young guard cell; MPC, mesophyll cell; GMC, guard mother cell; MMC, meristemoid mother cell; u.k., unknown.

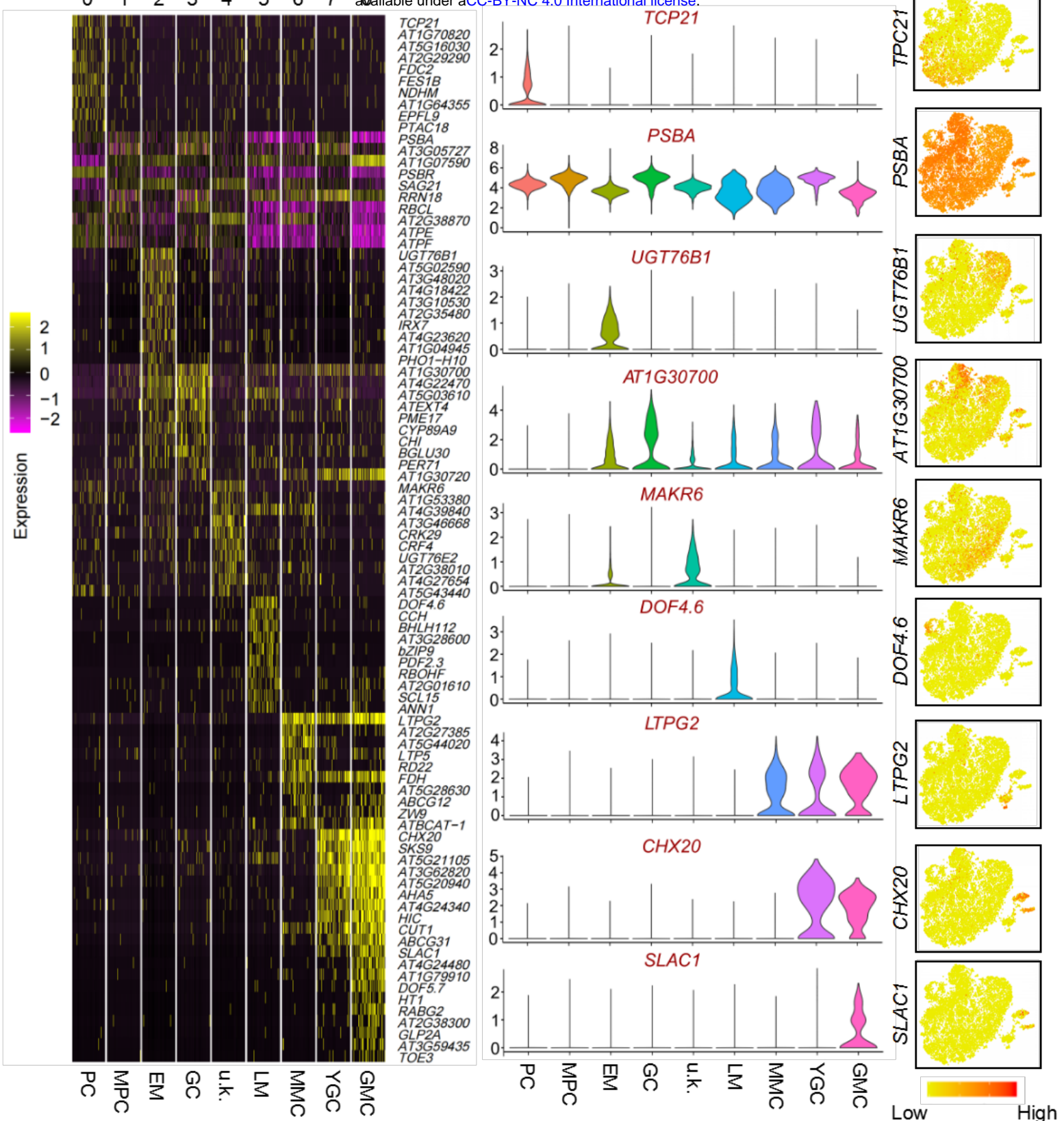


**Figure 2. Identification of novel marker genes for each cluster.** A, Heatmap of differentially expressed genes (DEGs). The top 5 genes and their relative expression levels in all sequenced cells are shown for each cluster. The color ranges from purple to yellow and represents the expression value of the marker genes from low to high. B, Violin plots of selected novel marker genes for each cluster. C, Feature plots of the expression distribution of selected novel marker genes. Expression levels for each cell are color-coded and superimposed on the tSNE plot. EM, early-stage meristemoid; GC, guard cell; PC, pavement cell; LM, late-stage meristemoid; YCG, young guard cell; MPC, mesophyll cell; GMC, guard mother cell; MMC, meristemoid mother cell; u.k., unknown.

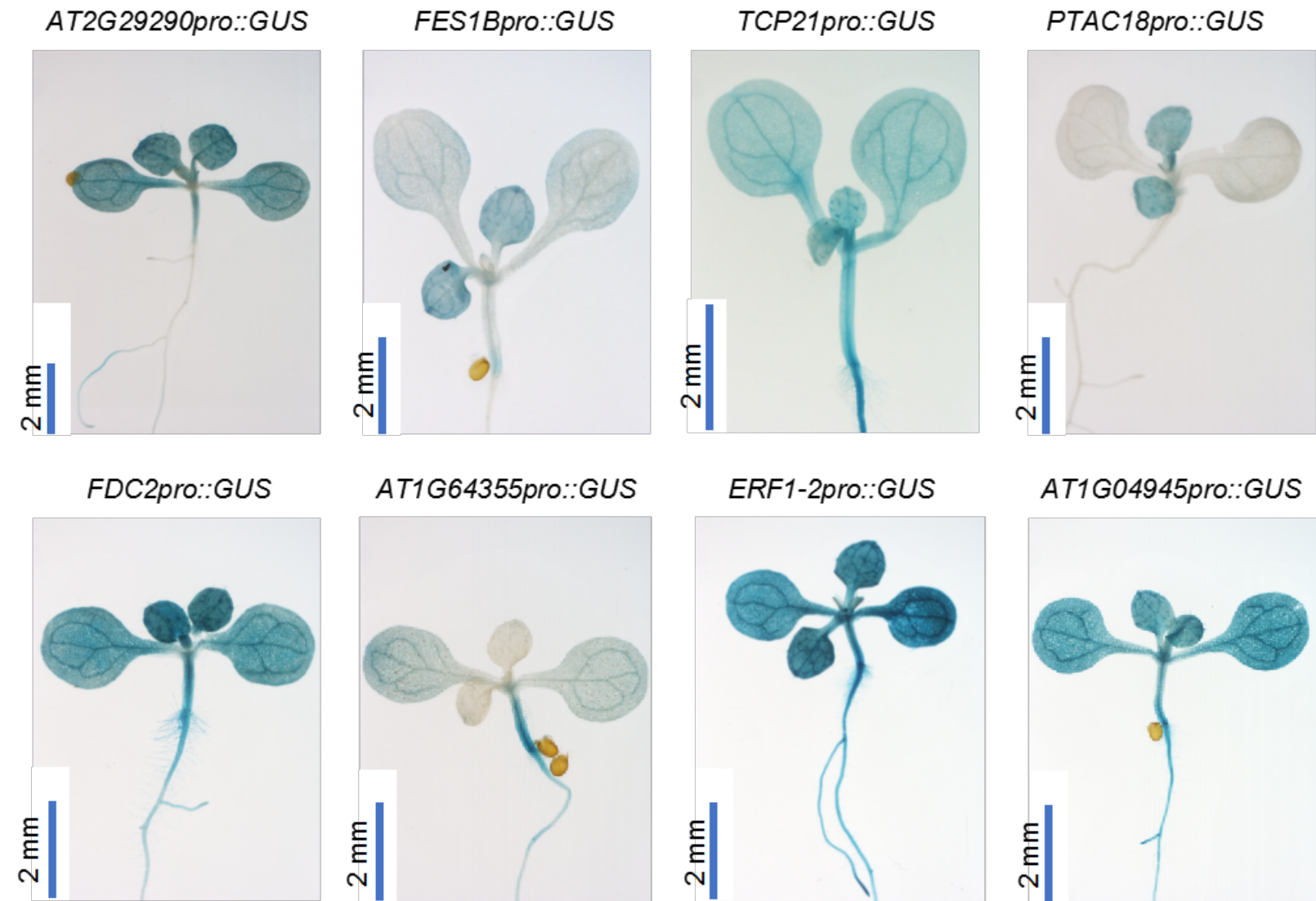


**Figure 3. Expression of selected marker genes in different tissues.** Transgenic plants expressing the GUS reporter gene driven by the promoters of the selected marker genes were generated to analyze their expression patterns. GUS signals were detected by staining. Scale bar, 2 mm is shown as a blue line.

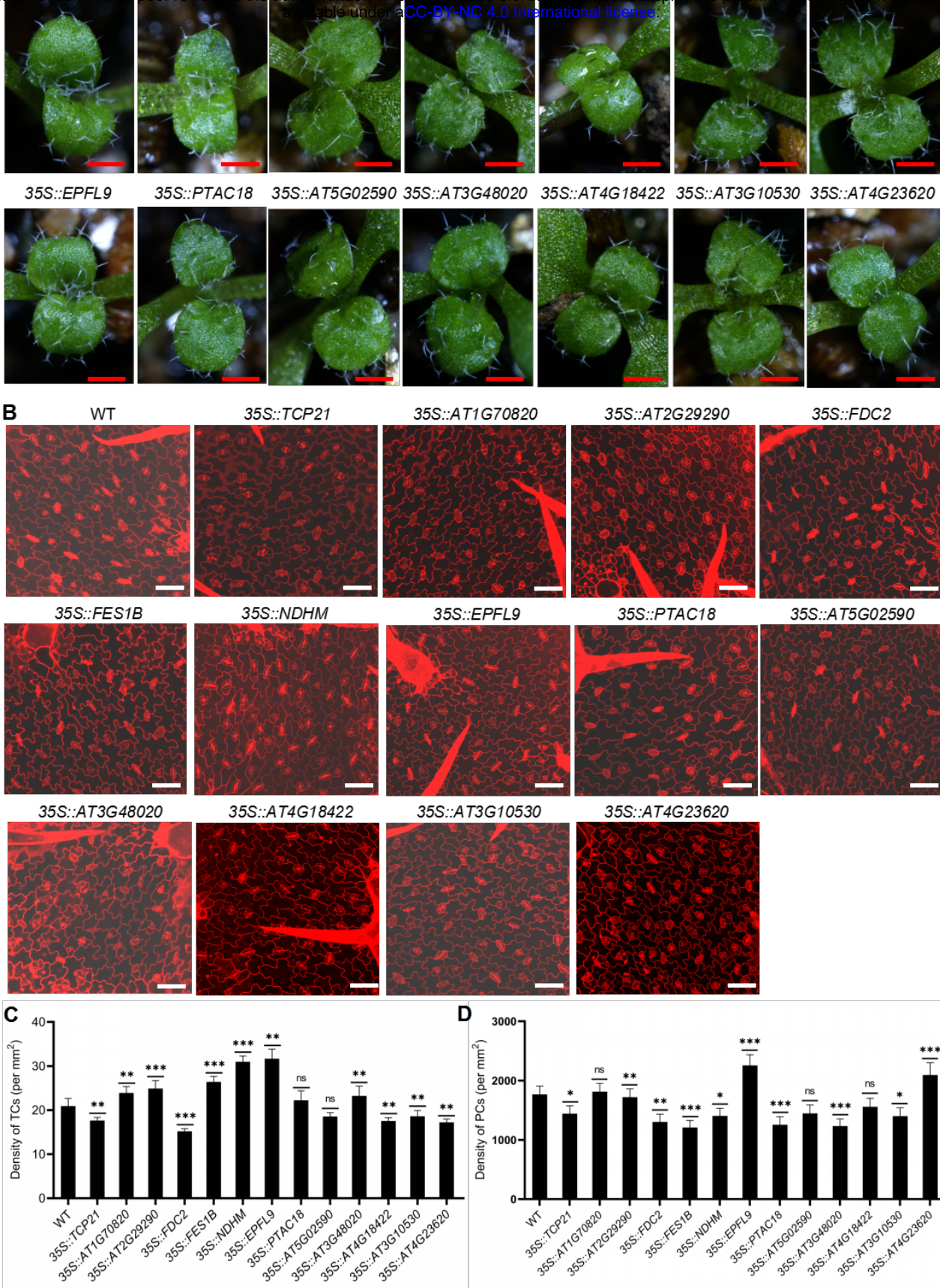


**Figure 4. Characterization of the potential roles of selected marker genes for pavement cells (PCs) and trichome cells (TCs).** A, Detection of the developmental status of trichomes in transgenic lines and wild-type (WT) seedlings. Scale bar (0.5 mm) is shown as a red line with a white background. B, Analysis of the developmental status of PCs in WT and transgenic lines. Samples were stained with propidium iodide, after which PCs were detected using a laser confocal microscope. Scale bar (50 m) is shown as a white line. C, TC density in the upper epidermis of two 3-day-old true leaves of WT and transgenic seedlings. D, PC density in the upper epidermis of 3-day-old true leaves of WT and transgenic seedlings. Data represent a mean  $\pm$  SD ( $n = 3$ ). Asterisks indicate a significant difference between transgenic and WT plants as determined using a Student's t-test. \* $P < 0.05$ , \*\* $P < 0.01$ , and \*\*\* $P < 0.001$ . ns, non-significant.

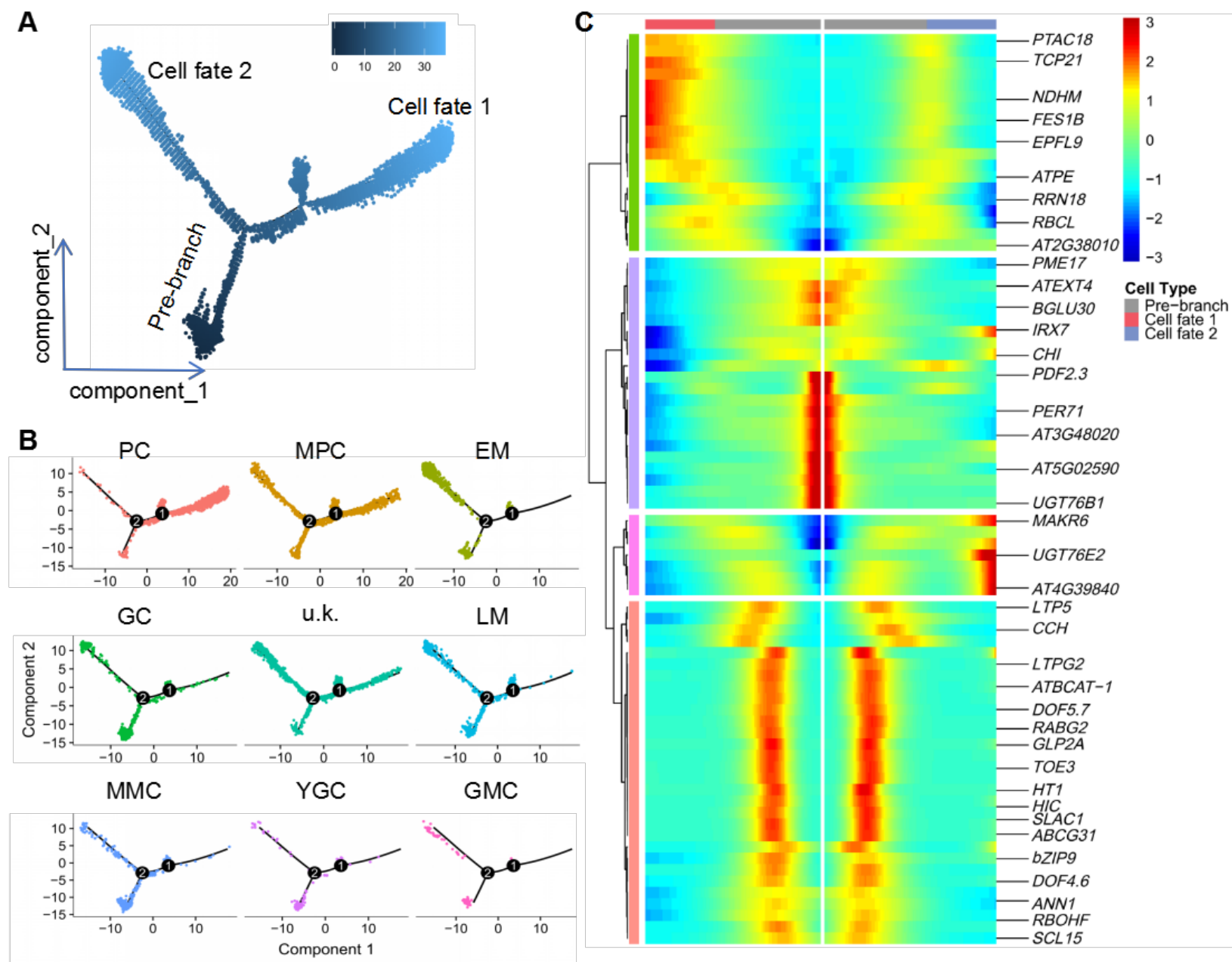


**Figure 5. Pseudo-time analysis reveals putative differentiation trajectories of different cell types.** A, Distribution of cells of each cluster on the pseudo-time trajectory. B, Distribution of cells of each cell type on the pseudo-time trajectory. C, Clustering and expression kinetics of the top 10 genes in all clusters along with a pseudo-time progression. EM, early-stage meristemoid; GC, guard cell; PC, pavement cell; LM, late-stage meristemoid; YCG, young guard cell; MPC, mesophyll cell; GMC, guard mother cell; MMC, meristemoid mother cell; u.k., unknown.

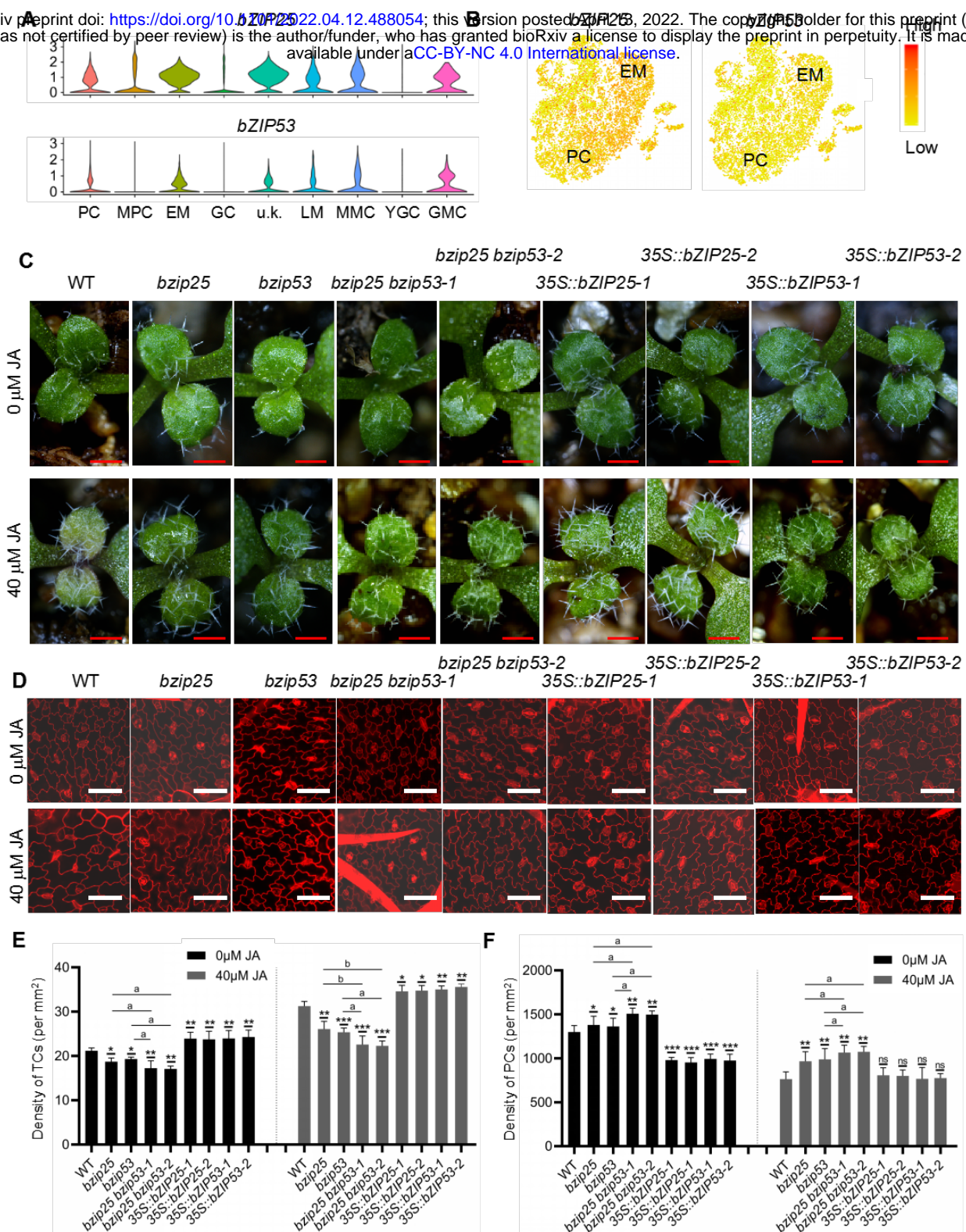


**Figure 6. *bZIP25* and *bZIP53* positively regulate trichome cell (TC) development and negatively regulate pavement cell (PC) development.** A, Violin plots showing the expression of *bZIP25* and *bZIP53* in EMs and PCs. B, Feature plots showing the expression of *bZIP25* and *bZIP53* in EMs and PCs. C, Representative photographs of the upper epidermis of 3-day-old true leaves of WT, *bzip25*, *bzip53*, *bzip25 bzip53*, *35S::bZIP25* and *35S::bZIP53* plants subjected to 0 (control) and 40 M jasmonic acid (JA) treatments. Bar, 500 m. D, Representative photographs of PCs in the upper epidermis of 3-day-old true leaves of WT, *bzip25*, *bzip53*, *bzip25 bzip53*, *35S::bZIP25* and *35S::bZIP53* plants subjected to 0 (control) and 40 M jasmonic acid (JA) treatments. The samples were treated by propidium iodide (PI) staining to show the cell wall. Bar, 50 m. (E-F) Density of TCs (E) and density of PCs (F) in the upper epidermis of two 3-day-old true leaves of WT, *bzip25*, *bzip53*, *bzip25 bzip53*, *35S::bZIP25* and *35S::bZIP53* plants subjected to 0 and 40 M JA treatments. Data represent a mean  $\pm$  SD ( $n = 3$ ). Asterisks indicate a significant difference between mutant and WT, and between overexpression lines and WT as determined using a Student's t-test. \* $P < 0.05$ , \*\* $P < 0.01$ , and \*\*\* $P < 0.001$ . ns, non-significant. Letters indicate a significant difference between single mutant and double mutant as determined using a Student's t-test. a  $P < 0.05$ , b  $P < 0.01$ .

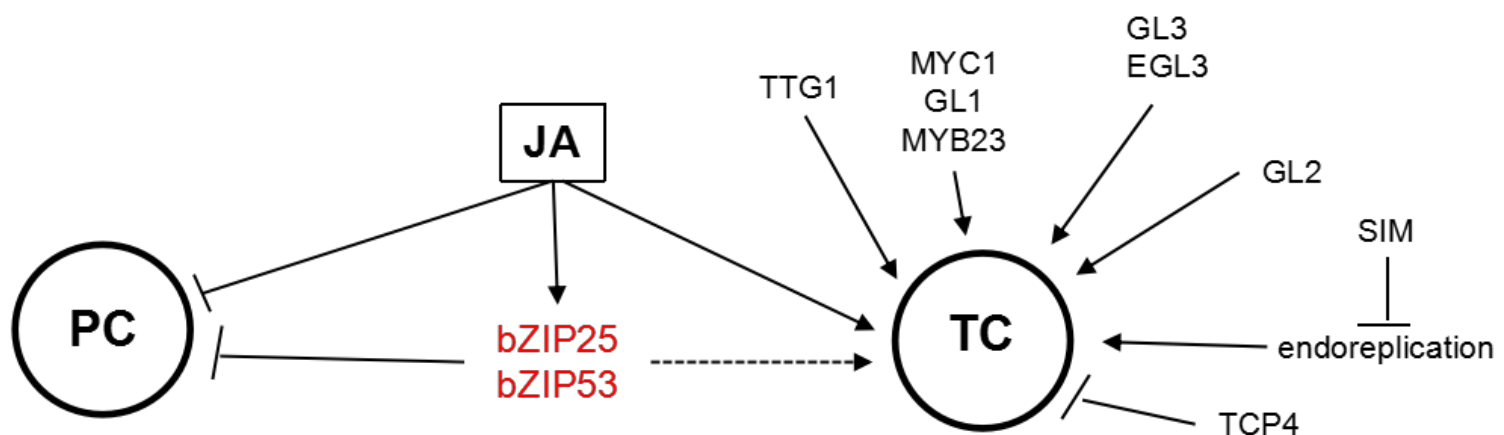


**Figure 7. Model of the transcription factor network, including bZIP25 and bZIP53, in regulating TC and PC development.** The fate of a TC is regulated by a series of critical transcription factors, including TTG1, GL2, MYC1, GL3, SIM, and TCPs, as well as others. JA positively promotes the development of TC but inhibits the differentiation of PC. bZIP25 and bZIP53, in response to JA, negatively regulate the fate of a PC and may positively promote the differentiation of a TC.

## Parsed Citations

Adrian J, Chang J, Ballenger CE, Bargmann BO, Alassimone J, Davies KA, Lau OS, Matos JL, Hachez C, Lanctot A, Vaten A, Birnbaum KD, Bergmann DC (2015) Transcriptome dynamics of the stomatal lineage: birth, amplification, and termination of a self-renewing population. *Dev Cell* 33: 107-118  
Google Scholar: [Author Only](#) [Title Only](#) [Author and Title](#)

Akhtar MQ, Qamar N, Yadav P, Kulkarni P, Kumar A, Shasany AK (2017) Comparative glandular trichome transcriptome-based gene characterization reveals reasons for differential (-)-menthol biosynthesis in *Mentha* species. *Physiol Plant* 160: 128-141  
Google Scholar: [Author Only](#) [Title Only](#) [Author and Title](#)

Ambrose JC, Shoji T, Kotzer AM, Pighin JA, Wasteneys GO (2007) The *Arabidopsis* CLASP gene encodes a microtubule-associated protein involved in cell expansion and division. *Plant Cell* 19: 2763-2775  
Google Scholar: [Author Only](#) [Title Only](#) [Author and Title](#)

Armour WJ, Barton DA, Law AM, Overall RL (2015) Differential Growth in Periclinal and Anticlinal Walls during Lobe Formation in *Arabidopsis* Cotyledon Pavement Cells. *Plant Cell* 27: 2484-2500  
Google Scholar: [Author Only](#) [Title Only](#) [Author and Title](#)

Bali S, Jamwal VL, Kohli SK, Kaur P, Tejpal R, Bhalla V, Ohri P, Gandhi SG, Bhardwaj R, Al-Huqail AA, Siddiqui MH, Ali HM, Ahmad P (2019) Jasmonic acid application triggers detoxification of lead (Pb) toxicity in tomato through the modifications of secondary metabolites and gene expression. *Chemosphere* 235: 734-748  
Google Scholar: [Author Only](#) [Title Only](#) [Author and Title](#)

Balkunde R, Pesch M, Hulskamp M (2010) Trichome patterning in *Arabidopsis thaliana* from genetic to molecular models. *Curr Top Dev Biol* 91: 299-321  
Google Scholar: [Author Only](#) [Title Only](#) [Author and Title](#)

Bar M, Ori N (2014) Leaf development and morphogenesis. *Development* 141: 4219-4230  
Google Scholar: [Author Only](#) [Title Only](#) [Author and Title](#)

Boughton AJ, Hoover K, Felton GW (2005) Methyl jasmonate application induces increased densities of glandular trichomes on tomato, *Lycopersicon esculentum*. *J Chem Ecol* 31: 2211-2216  
Google Scholar: [Author Only](#) [Title Only](#) [Author and Title](#)

Breuer C, Kawamura A, Ichikawa T, Tominaga-Wada R, Wada T, Kondou Y, Muto S, Matsui M, Sugimoto K (2009) The trihelix transcription factor GTL1 regulates ploidy-dependent cell growth in the *Arabidopsis* trichome. *Plant Cell* 21: 2307-2322  
Google Scholar: [Author Only](#) [Title Only](#) [Author and Title](#)

Byrne M, Timmermans M, Kidner C, Martienssen R (2001) Development of leaf shape. *Curr Opin Plant Biol* 4: 38-43  
Google Scholar: [Author Only](#) [Title Only](#) [Author and Title](#)

Caarls L, Elberse J, Awwanah M, Ludwig NR, de Vries M, Zeilmaker T, Van Wees SCM, Schuurink RC, Van den Ackerveken G (2017) *Arabidopsis* JASMONATE-INDUCED OXYGENASES down-regulate plant immunity by hydroxylation and inactivation of the hormone jasmonic acid. *Proc Natl Acad Sci U S A* 114: 6388-6393  
Google Scholar: [Author Only](#) [Title Only](#) [Author and Title](#)

Canet JV, Dobon A, Fajmonova J, Tornero P (2012) The BLADE-ON-PETIOLE genes of *Arabidopsis* are essential for resistance induced by methyl jasmonate. *BMC Plant Biol* 12: 199  
Google Scholar: [Author Only](#) [Title Only](#) [Author and Title](#)

Chen C, Liu M, Jiang L, Liu X, Zhao J, Yan S, Yang S, Ren H, Liu R, Zhang X (2014) Transcriptome profiling reveals roles of meristem regulators and polarity genes during fruit trichome development in cucumber (*Cucumis sativus* L.). *J Exp Bot* 65: 4943-4958  
Google Scholar: [Author Only](#) [Title Only](#) [Author and Title](#)

Chini A, Fonseca S, Fernandez G, Adie B, Chico JM, Lorenzo O, Garcia-Casado G, Lopez-Vidriero I, Lozano FM, Ponce MR, Micol JL, Solano R (2007) The JAZ family of repressors is the missing link in jasmonate signalling. *Nature* 448: 666-+  
Google Scholar: [Author Only](#) [Title Only](#) [Author and Title](#)

Chung HS, Howe GA (2009) A critical role for the TIFY motif in repression of jasmonate signaling by a stabilized splice variant of the JASMONATE ZIM-domain protein JAZ10 in *Arabidopsis*. *Plant Cell* 21: 131-145  
Google Scholar: [Author Only](#) [Title Only](#) [Author and Title](#)

Churchman ML, Brown ML, Kato N, Kirik V, Hulskamp M, Inze D, De Veylder L, Walker JD, Zheng Z, Oppenheimer DG, Gwin T, Churchman J, Larkin JC (2006) SIAMESE, a plant-specific cell cycle regulator, controls endoreplication onset in *Arabidopsis thaliana*. *Plant Cell* 18: 3145-3157  
Google Scholar: [Author Only](#) [Title Only](#) [Author and Title](#)

Clarke JD, Aarts N, Feys BJ, Dong X, Parker JE (2001) Constitutive disease resistance requires EDS1 in the *Arabidopsis* mutants

**cpr1 and cpr6 and is partially EDS1-dependent in cpr5. Plant J 26: 409-420**

Google Scholar: [Author Only](#) [Title Only](#) [Author and Title](#)

**Delker C, Zolman BK, Miersch O, Wasternack C (2007) Jasmonate biosynthesis in *Arabidopsis thaliana* requires peroxisomal beta-oxidation enzymes--additional proof by properties of pex6 and aim1. Phytochemistry 68: 1642-1650**

Google Scholar: [Author Only](#) [Title Only](#) [Author and Title](#)

**Efroni I, Blum E, Goldshmidt A, Eshed Y (2008) A protracted and dynamic maturation schedule underlies *Arabidopsis* leaf development. Plant Cell 20: 2293-2306**

Google Scholar: [Author Only](#) [Title Only](#) [Author and Title](#)

**Eng RC, Schneider R, Matz TW, Carter R, Ehrhardt DW, Jonsson H, Nikoloski Z, Sampathkumar A (2021) KATANIN and CLASP function at different spatial scales to mediate microtubule response to mechanical stress in *Arabidopsis* cotyledons. Curr Biol 31: 3262-+**

Google Scholar: [Author Only](#) [Title Only](#) [Author and Title](#)

**Esch JJ, Chen M, Sanders M, Hillestad M, Ndkium S, Idelkope B, Neizer J, Marks MD (2003) A contradictory GLABRA3 allele helps define gene interactions controlling trichome development in *Arabidopsis*. Development 130: 5885-5894**

Google Scholar: [Author Only](#) [Title Only](#) [Author and Title](#)

**Esch JJ, Chen MA, Hillestad M, Marks MD (2004) Comparison of TRY and the closely related At1g01380 gene in controlling *Arabidopsis* trichome patterning. Plant J 40: 860-869**

Google Scholar: [Author Only](#) [Title Only](#) [Author and Title](#)

**Fleming AJ (2005) The control of leaf development. New Phytol 166: 9-20**

Google Scholar: [Author Only](#) [Title Only](#) [Author and Title](#)

**Fu Y, Gu Y, Zheng Z, Wasteneys G, Yang Z (2005) *Arabidopsis* interdigitating cell growth requires two antagonistic pathways with opposing action on cell morphogenesis. Cell 120: 687-700**

Google Scholar: [Author Only](#) [Title Only](#) [Author and Title](#)

**Gan L, Xia K, Chen JG, Wang S (2011) Functional characterization of TRICHOMELESS2, a new single-repeat R3 MYB transcription factor in the regulation of trichome patterning in *Arabidopsis*. BMC Plant Biol 11: 176**

Google Scholar: [Author Only](#) [Title Only](#) [Author and Title](#)

**Grebe M (2012) The patterning of epidermal hairs in *Arabidopsis*--updated. Curr Opin Plant Biol 15: 31-37**

Google Scholar: [Author Only](#) [Title Only](#) [Author and Title](#)

**Gupta A, Bhardwaj M, Tran LP (2021) JASMONATE ZIM-DOMAIN Family Proteins: Important Nodes in Jasmonic Acid-Abscisic Acid Crosstalk for Regulating Plant Response to Drought. Curr Protein Pept Sci 22: 759-766**

Google Scholar: [Author Only](#) [Title Only](#) [Author and Title](#)

**Hao J, Cao W, Huang J, Zou X, Han ZG (2019) Optimal Gene Filtering for Single-Cell data (OGFSC)-a gene filtering algorithm for single-cell RNA-seq data. Bioinformatics 35: 2602-2609**

Google Scholar: [Author Only](#) [Title Only](#) [Author and Title](#)

**Hauser MT (2014) Molecular basis of natural variation and environmental control of trichome patterning. Front Plant Sci 5: 320**

Google Scholar: [Author Only](#) [Title Only](#) [Author and Title](#)

**Herman PL, Marks MD (1989) Trichome Development in *Arabidopsis thaliana*. II. Isolation and Complementation of the GLABROUS1 Gene. Plant Cell 1: 1051-1055**

Google Scholar: [Author Only](#) [Title Only](#) [Author and Title](#)

**Hilscher J, Schlotterer C, Hauser MT (2009) A single amino acid replacement in ETC2 shapes trichome patterning in natural *Arabidopsis* populations. Curr Biol 19: 1747-1751**

Google Scholar: [Author Only](#) [Title Only](#) [Author and Title](#)

**Hulskamp M, Misra S, Jurgens G (1994) Genetic dissection of trichome cell development in *Arabidopsis*. Cell 76: 555-566**

Google Scholar: [Author Only](#) [Title Only](#) [Author and Title](#)

**Ilgenfritz H, Bouyer D, Schnittger A, Mathur J, Kirik V, Schwab B, Chua NH, Jurgens G, Hulskamp M (2003) The *Arabidopsis* STICHEL gene is a regulator of trichome branch number and encodes a novel protein. Plant Physiol 131: 643-655**

Google Scholar: [Author Only](#) [Title Only](#) [Author and Title](#)

**Ishida T, Kurata T, Okada K, Wada T (2008) A genetic regulatory network in the development of trichomes and root hairs. Annu Rev Plant Biol 59: 365-386**

Google Scholar: [Author Only](#) [Title Only](#) [Author and Title](#)

**Kalve S, De Vos D, Beemster GT (2014) Leaf development: a cellular perspective. Front Plant Sci 5: 362**

Google Scholar: [Author Only](#) [Title Only](#) [Author and Title](#)

**Kim JY, Symeonidi E, Pang TY, Denyer T, Weidauer D, Bezrutczyk M, Miras M, Zollner N, Hartwig T, Wudick MM, Lercher M, Chen LQ, Timmermans MCP, Frommer WB (2021) Distinct identities of leaf phloem cells revealed by single cell transcriptomics. *Plant Cell* 33: 511-530**

Google Scholar: [Author Only](#) [Title Only](#) [Author and Title](#)

**Kirik V, Lee MM, Wester K, Herrmann U, Zheng Z, Oppenheimer D, Schiefelbein J, Hulskamp M (2005) Functional diversification of MYB23 and GL1 genes in trichome morphogenesis and initiation. *Development* 132: 1477-1485**

Google Scholar: [Author Only](#) [Title Only](#) [Author and Title](#)

**Kirik V, Schnittger A, Radchuk V, Adler K, Hulskamp M, Baumlein H (2001) Ectopic expression of the *Arabidopsis* AtMYB23 gene induces differentiation of trichome cells. *Dev Biol* 235: 366-377**

Google Scholar: [Author Only](#) [Title Only](#) [Author and Title](#)

**Kirik V, Simon M, Hulskamp M, Schiefelbein J (2004) The ENHANCER OF TRY AND CPC1 gene acts redundantly with TRPTYCHON and CAPRICE in trichome and root hair cell patterning in *Arabidopsis*. *Dev Biol* 268: 506-513**

Google Scholar: [Author Only](#) [Title Only](#) [Author and Title](#)

**Kirik V, Simon M, Wester K, Schiefelbein J, Hulskamp M (2004) ENHANCER of TRY and CPC 2 (ETC2) reveals redundancy in the region-specific control of trichome development of *Arabidopsis*. *Plant Mol Biol* 55: 389-398**

Google Scholar: [Author Only](#) [Title Only](#) [Author and Title](#)

**Koornneef M (1981) The complex syndrome of TTG mutants. *arabid.inf.serv***

Google Scholar: [Author Only](#) [Title Only](#) [Author and Title](#)

**Larkin JC, Oppenheimer DG, Lloyd AM, Paparozzi ET, Marks MD (1994) Roles of the GLABROUS1 and TRANSPARENT TESTA GLABRA Genes in *Arabidopsis* Trichome Development. *Plant Cell* 6: 1065-1076**

Google Scholar: [Author Only](#) [Title Only](#) [Author and Title](#)

**Larkin JC, Oppenheimer DG, Marks MD (1994) The GL1 gene and the trichome developmental pathway in *Arabidopsis thaliana*. *Results Probl Cell Differ* 20: 259-275**

Google Scholar: [Author Only](#) [Title Only](#) [Author and Title](#)

**Larkin JC, Young N, Prigge M, Marks MD (1996) The control of trichome spacing and number in *Arabidopsis*. *Development* 122: 997-1005**

Google Scholar: [Author Only](#) [Title Only](#) [Author and Title](#)

**LeBrasseur ND, MacIntosh GC, Perez-Amador MA, Saitoh M, Green PJ (2002) Local and systemic wound-induction of RNase and nuclease activities in *Arabidopsis*: RNS1 as a marker for a JA-independent systemic signaling pathway. *Plant J* 29: 393-403**

Google Scholar: [Author Only](#) [Title Only](#) [Author and Title](#)

**Li L, Zhao Y, McCaig BC, Wingerd BA, Wang J, Whalon ME, Pichersky E, Howe GA (2004) The tomato homolog of CORONATINE-INSENSITIVE1 is required for the maternal control of seed maturation, jasmonate-signaled defense responses, and glandular trichome development. *Plant Cell* 16: 126-143**

Google Scholar: [Author Only](#) [Title Only](#) [Author and Title](#)

**Liang H, Zhang Y, Martinez P, Rasmussen CG, Xu T, Yang Z (2018) The Microtubule-Associated Protein IQ67 DOMAIN5 Modulates Microtubule Dynamics and Pavement Cell Shape. *Plant Physiol* 177: 1555-1568**

Google Scholar: [Author Only](#) [Title Only](#) [Author and Title](#)

**Lin D, Cao L, Zhou Z, Zhu L, Ehrhardt D, Yang Z, Fu Y (2013) Rho GTPase signaling activates microtubule severing to promote microtubule ordering in *Arabidopsis*. *Curr Biol* 23: 290-297**

Google Scholar: [Author Only](#) [Title Only](#) [Author and Title](#)

**Liu Q, Liang Z, Feng D, Jiang SJ, Wang YF, Du ZY, Li RX, Hu GH, Zhang PX, Ma YF, Lohmann JU, Gu XF (2021) Transcriptional landscape of rice roots at the single-cell resolution. *Mol Plant* 14: 384-394**

Google Scholar: [Author Only](#) [Title Only](#) [Author and Title](#)

**Liu Z, Wang J, Zhou Y, Zhang Y, Qin A, Yu X, Zhao Z, Wu R, Guo C, Bawa G, Rochaix JD, Sun X (2022) Identification of Novel Regulators Required for Early Development of Vein Pattern in the Cotyledons by Single-cell RNA-seq. *Plant J***

Google Scholar: [Author Only](#) [Title Only](#) [Author and Title](#)

**Liu Z, Zhou Y, Guo J, Li J, Tian Z, Zhu Z, Wang J, Wu R, Zhang B, Hu Y, Sun Y, Shangguan Y, Li W, Li T, Hu Y, Guo C, Rochaix JD, Miao Y, Sun X (2020) Global Dynamic Molecular Profiles of Stomatal Lineage Cell Development by Single-Cell RNA Sequencing. *Mol Plant***

Google Scholar: [Author Only](#) [Title Only](#) [Author and Title](#)

**Lloyd AM, Schena M, Walbot V, Davis RW (1994) Epidermal cell fate determination in *Arabidopsis*: patterns defined by a steroid-inducible regulator. *Science* 266: 436-439**

Google Scholar: [Author Only](#) [Title Only](#) [Author and Title](#)

**Lu D, Wang T, Persson S, Mueller-Roeber B, Schippers JH (2014) Transcriptional control of ROS homeostasis by KUODA1 regulates cell expansion during leaf development. *Nat Commun* 5: 3767**

Google Scholar: [Author Only](#) [Title Only](#) [Author and Title](#)

**Macosko EZ, Basu A, Satija R, Nemesh J, Shekhar K, Goldman M, Tirosh I, Bialas AR, Kamitaki N, Martersteck EM, Trombetta JJ, Weitz DA, Sanes JR, Shalek AK, Regev A, McCarroll SA (2015) Highly Parallel Genome-wide Expression Profiling of Individual Cells Using Nanoliter Droplets. *Cell* 161: 1202-1214**

Google Scholar: [Author Only](#) [Title Only](#) [Author and Title](#)

**Marks MD (1997) Molecular Genetic Analysis of Trichome Development in *Arabidopsis*. *Annu Rev Plant Physiol Plant Mol Biol* 48: 137-163**

Google Scholar: [Author Only](#) [Title Only](#) [Author and Title](#)

**Marks MD, Betancur L, Gilding E, Chen F, Bauer S, Wenger JP, Dixon RA, Haigler CH (2008) A new method for isolating large quantities of *Arabidopsis* trichomes for transcriptome, cell wall and other types of analyses. *Plant J* 56: 483-492**

Google Scholar: [Author Only](#) [Title Only](#) [Author and Title](#)

**Marks MD, Feldmann KA (1989) Trichome Development in *Arabidopsis thaliana*. I. T-DNA Tagging of the GLABROUS1 Gene. *Plant Cell* 1: 1043-1050**

Google Scholar: [Author Only](#) [Title Only](#) [Author and Title](#)

**Marks MD, Wenger JP, Gilding E, Jilk R, Dixon RA (2009) Transcriptome analysis of *Arabidopsis* wild-type and *gl3-sst* sim trichomes identifies four additional genes required for trichome development. *Mol Plant* 2: 803-822**

Google Scholar: [Author Only](#) [Title Only](#) [Author and Title](#)

**Morohashi K, Zhao M, Yang M, Read B, Lloyd A, Lamb R, Grotewold E (2007) Participation of the *Arabidopsis* bHLH factor GL3 in trichome initiation regulatory events. *Plant Physiol* 145: 736-746**

Google Scholar: [Author Only](#) [Title Only](#) [Author and Title](#)

**Noir S, Bomer M, Takahashi N, Ishida T, Tsui TL, Balbi V, Shanahan H, Sugimoto K, Devoto A (2013) Jasmonate Controls Leaf Growth by Repressing Cell Proliferation and the Onset of Endoreduplication while Maintaining a Potential Stand-By Mode. *Plant Physiol* 161: 1930-1951**

Google Scholar: [Author Only](#) [Title Only](#) [Author and Title](#)

**Oppenheimer DG, Herman PL, Sivakumaran S, Esch J, Marks MD (1991) A *myb* gene required for leaf trichome differentiation in *Arabidopsis* is expressed in stipules. *Cell* 67: 483-493**

Google Scholar: [Author Only](#) [Title Only](#) [Author and Title](#)

**Overmyer K, Tuominen H, Kettunen R, Betz C, Langebartels C, Sandermann H, Jr., Kangasjarvi J (2000) Ozone-sensitive *arabidopsis rcd1* mutant reveals opposite roles for ethylene and jasmonate signaling pathways in regulating superoxide-dependent cell death. *Plant Cell* 12: 1849-1862**

Google Scholar: [Author Only](#) [Title Only](#) [Author and Title](#)

**Pathuri IP, Zellerhoff N, Schaffrath U, Hensel G, Kumlehn J, Kogel KH, Eichmann R, Huckelhoven R (2008) Constitutively activated barley ROPs modulate epidermal cell size, defense reactions and interactions with fungal leaf pathogens. *Plant Cell Rep* 27: 1877-1887**

Google Scholar: [Author Only](#) [Title Only](#) [Author and Title](#)

**Payne CT, Zhang F, Lloyd AM (2000) GL3 encodes a bHLH protein that regulates trichome development in *arabidopsis* through interaction with GL1 and TTG1. *Genetics* 156: 1349-1362**

Google Scholar: [Author Only](#) [Title Only](#) [Author and Title](#)

**Payne T, Clement J, Arnold D, Lloyd A (1999) Heterologous *myb* genes distinct from GL1 enhance trichome production when overexpressed in *Nicotiana tabacum*. *Development* 126: 671-682**

Google Scholar: [Author Only](#) [Title Only](#) [Author and Title](#)

**Peng S, Huang S, Liu Z, Feng H (2019) Mutation of ACX1, a Jasmonic Acid Biosynthetic Enzyme, Leads to Petal Degeneration in Chinese Cabbage (*Brassica campestris* ssp. *pekinensis*). *Int J Mol Sci* 20**

Google Scholar: [Author Only](#) [Title Only](#) [Author and Title](#)

**Pesch M, Hulskamp M (2009) One, two, three...models for trichome patterning in *Arabidopsis*? *Curr Opin Plant Biol* 12: 587-592**

Google Scholar: [Author Only](#) [Title Only](#) [Author and Title](#)

**Pesch M, Hulskamp M (2011) Role of TRIPTYCHON in trichome patterning in *Arabidopsis*. *BMC Plant Biol* 11: 130**

Google Scholar: [Author Only](#) [Title Only](#) [Author and Title](#)

**Pesch M, Schultheiss I, Digiuni S, Uhrig JF, Hulskamp M (2013) Mutual control of intracellular localisation of the patterning proteins AtMYC1, GL1 and TRY/CPC in *Arabidopsis*. *Development* 140: 3456-3467**

Google Scholar: [Author Only](#) [Title Only](#) [Author and Title](#)

**Qi T, Song S, Ren Q, Wu D, Huang H, Chen Y, Fan M, Peng W, Ren C, Xie D (2011) The Jasmonate-ZIM-domain proteins interact with the WD-Repeat/bHLH/MYB complexes to regulate Jasmonate-mediated anthocyanin accumulation and trichome initiation in *Arabidopsis thaliana*. *Plant Cell* 23: 1795-1814**

Google Scholar: [Author Only](#) [Title Only](#) [Author and Title](#)

**Quint M, Ito H, Zhang W, Gray WM (2005) Characterization of a novel temperature-sensitive allele of the CUL1/AXR6 subunit of SCF ubiquitin-ligases. *Plant J* 43: 371-383**

Google Scholar: [Author Only](#) [Title Only](#) [Author and Title](#)

**Rerie WG, Feldmann KA, Marks MD (1994) The GLABRA2 gene encodes a homeo domain protein required for normal trichome development in *Arabidopsis*. *Genes Dev* 8: 1388-1399**

Google Scholar: [Author Only](#) [Title Only](#) [Author and Title](#)

**Rheume BA, Jereen A, Bolisetty M, Sajid MS, Yang Y, Renna K, Sun L, Robson P, Trakhtenberg EF (2018) Single cell transcriptome profiling of retinal ganglion cells identifies cellular subtypes. *Nat Commun* 9: 2759**

Google Scholar: [Author Only](#) [Title Only](#) [Author and Title](#)

**Schnittger A, Folkers U, Schwab B, Jurgens G, Hulskamp M (1999) Generation of a spacing pattern: the role of triptychon in trichome patterning in *Arabidopsis*. *Plant Cell* 11: 1105-1116**

Google Scholar: [Author Only](#) [Title Only](#) [Author and Title](#)

**Serrano-Ron L, Perez-Garcia P, Sanchez-Corronero A, Gude I, Cabrera J, Ip PL, Birnbaum KD, Moreno-Risueno MA (2021) Reconstruction of lateral root formation through single-cell RNA sequencing reveals order of tissue initiation. *Mol Plant* 14: 1362-1378**

Google Scholar: [Author Only](#) [Title Only](#) [Author and Title](#)

**Sun XW, Xu DR, Liu ZX, Kleine T, Leister D (2016) Functional relationship between mTERF4 and GUN1 in retrograde signaling. *J Exp Bot* 67: 3909-3924**

Google Scholar: [Author Only](#) [Title Only](#) [Author and Title](#)

**Szymanski DB, Jilk RA, Pollock SM, Marks MD (1998) Control of GL2 expression in *Arabidopsis* leaves and trichomes. *Development* 125: 1161-1171**

Google Scholar: [Author Only](#) [Title Only](#) [Author and Title](#)

**Thines B, Katsir L, Melotto M, Niu Y, Mandaokar A, Liu G, Nomura K, He SY, Howe GA, Browse J (2007) JAZ repressor proteins are targets of the SCF(CO1) complex during jasmonate signalling. *Nature* 448: 661-665**

Google Scholar: [Author Only](#) [Title Only](#) [Author and Title](#)

**Tian H, Qi T, Li Y, Wang C, Ren C, Song S, Huang H (2016) Regulation of the WD-repeat/bHLH/MYB complex by gibberellin and jasmonate. *Plant Signal Behav* 11: e1204061**

Google Scholar: [Author Only](#) [Title Only](#) [Author and Title](#)

**Tian H, Wang X, Guo H, Cheng Y, Hou C, Chen JG, Wang S (2017) NTL8 Regulates Trichome Formation in *Arabidopsis* by Directly Activating R3 MYB Genes TRY and TCL1. *Plant Physiol* 174: 2363-2375**

Google Scholar: [Author Only](#) [Title Only](#) [Author and Title](#)

**Trapnell C, Cacchiarelli D, Grimsby J, Pokharel P, Li S, Morse M, Lennon NJ, Livak KJ, Mikkelsen TS, Rinn JL (2014) The dynamics and regulators of cell fate decisions are revealed by pseudotemporal ordering of single cells. *Nat Biotechnol* 32: 381-386**

Google Scholar: [Author Only](#) [Title Only](#) [Author and Title](#)

**Traw MB, Bergelson J (2003) Interactive effects of jasmonic acid, salicylic acid, and gibberellin on induction of trichomes in *Arabidopsis*. *Plant Physiol* 133: 1367-1375**

Google Scholar: [Author Only](#) [Title Only](#) [Author and Title](#)

**Vadde BVL, Challa KR, Sunkara P, Hegde AS, Nath U (2019) The TCP4 Transcription Factor Directly Activates TRICHOMELESS1 and 2 and Suppresses Trichome Initiation. *Plant Physiol* 181: 1587-1599**

Google Scholar: [Author Only](#) [Title Only](#) [Author and Title](#)

**Wada T, Tachibana T, Shimura Y, Okada K (1997) Epidermal cell differentiation in *Arabidopsis* determined by a Myb homolog, CPC. *Science* 277: 1113-1116**

Google Scholar: [Author Only](#) [Title Only](#) [Author and Title](#)

**Walker AR, Davison PA, Bolognesi-Winfield AC, James CM, Srinivasan N, Blundell TL, Esch JJ, Marks MD, Gray JC (1999) The TRANSPARENT TESTA GLABRA1 locus, which regulates trichome differentiation and anthocyanin biosynthesis in *Arabidopsis*, encodes a WD40 repeat protein. *Plant Cell* 11: 1337-1350**

Google Scholar: [Author Only](#) [Title Only](#) [Author and Title](#)

**Walker JD, Oppenheimer DG, Concienne J, Larkin JC (2000) SIAMESE, a gene controlling the endoreduplication cell cycle in *Arabidopsis thaliana* trichomes. *Development* 127: 3931-3940**

Google Scholar: [Author Only](#) [Title Only](#) [Author and Title](#)

**Wang S, Hubbard L, Chang Y, Guo J, Schiefelbein J, Chen JG (2008) Comprehensive analysis of single-repeat R3 MYB proteins in epidermal cell patterning and their transcriptional regulation in *Arabidopsis*. *BMC Plant Biol* 8: 81**

Google Scholar: [Author Only](#) [Title Only](#) [Author and Title](#)

**Wang W, Wang Y, Zhang Q, Qi Y, Guo D (2009) Global characterization of *Artemisia annua* glandular trichome transcriptome using 454 pyrosequencing. *BMC Genomics* 10: 465**

Google Scholar: [Author Only](#) [Title Only](#) [Author and Title](#)

**Wen J, Li Y, Qi T, Gao H, Liu B, Zhang M, Huang H, Song S (2018) The C-terminal domains of *Arabidopsis* GL3/EGL3/TT8 interact with JAZ proteins and mediate dimeric interactions. *Plant Signal Behav* 13: e1422460**

Google Scholar: [Author Only](#) [Title Only](#) [Author and Title](#)

**Wendrich JR, Yang B, Vandamme N, Verstaen K, Smet W, Van de Velde C, Minne M, Wybouw B, Mor E, Arents HE, Nolf J, Van Duyse J, Van Isterdael G, Maere S, Saeys Y, De Rybel B (2020) Vascular transcription factors guide plant epidermal responses to limiting phosphate conditions. *Science* 370**

Google Scholar: [Author Only](#) [Title Only](#) [Author and Title](#)

**Wester K, Digiuni S, Geier F, Timmer J, Fleck C, Hulskamp M (2009) Functional diversity of R3 single-repeat genes in trichome development. *Development* 136: 1487-1496**

Google Scholar: [Author Only](#) [Title Only](#) [Author and Title](#)

**Wightman R, Chomicki G, Kumar M, Carr P, Turner SR (2013) SPIRAL2 determines plant microtubule organization by modulating microtubule severing. *Curr Biol* 23: 1902-1907**

Google Scholar: [Author Only](#) [Title Only](#) [Author and Title](#)

**Xie DX, Feys BF, James S, Nieto-Rostro M, Turner JG (1998) COI1: an *Arabidopsis* gene required for jasmonate-regulated defense and fertility. *Science* 280: 1091-1094**

Google Scholar: [Author Only](#) [Title Only](#) [Author and Title](#)

**Xu T, Wen M, Nagawa S, Fu Y, Chen JG, Wu MJ, Perrot-Rechenmann C, Friml J, Jones AM, Yang Z (2010) Cell surface- and rho GTPase-based auxin signaling controls cellular interdigitation in *Arabidopsis*. *Cell* 143: 99-110**

Google Scholar: [Author Only](#) [Title Only](#) [Author and Title](#)

**Yan T, Chen M, Shen Q, Li L, Fu X, Pan Q, Tang Y, Shi P, Lv Z, Jiang W, Ma YN, Hao X, Sun X, Tang K (2017) HOMEO DOMAIN PROTEIN 1 is required for jasmonate-mediated glandular trichome initiation in *Artemisia annua*. *New Phytol* 213: 1145-1155**

Google Scholar: [Author Only](#) [Title Only](#) [Author and Title](#)

**Yanagisawa M, Desyatova AS, Belteton SA, Mallery EL, Turner JA, Szymanski DB (2015) Patterning mechanisms of cytoskeletal and cell wall systems during leaf trichome morphogenesis. *Nat Plants* 1: 15014**

Google Scholar: [Author Only](#) [Title Only](#) [Author and Title](#)

**Yang C, Gao Y, Gao S, Yu G, Xiong C, Chang J, Li H, Ye Z (2015) Transcriptome profile analysis of cell proliferation molecular processes during multicellular trichome formation induced by tomato Wo (v) gene in tobacco. *Genom Data* 6: 173-174**

Google Scholar: [Author Only](#) [Title Only](#) [Author and Title](#)

**Yoo SD, Cho YH, Sheen J (2007) *Arabidopsis* mesophyll protoplasts: a versatile cell system for transient gene expression analysis. *Nat Protoc* 2: 1565-1572**

Google Scholar: [Author Only](#) [Title Only](#) [Author and Title](#)

**Yoshida Y, Sano R, Wada T, Takabayashi J, Okada K (2009) Jasmonic acid control of GLABRA3 links inducible defense and trichome patterning in *Arabidopsis*. *Development* 136: 1039-1048**

Google Scholar: [Author Only](#) [Title Only](#) [Author and Title](#)

**Zhang F, Gonzalez A, Zhao M, Payne CT, Lloyd A (2003) A network of redundant bHLH proteins functions in all TTG1-dependent pathways of *Arabidopsis*. *Development* 130: 4859-4869**

Google Scholar: [Author Only](#) [Title Only](#) [Author and Title](#)

**Zhang TQ, Xu ZG, Shang GD, Wang JW (2019) A Single-Cell RNA Sequencing Profiles the Developmental Landscape of *Arabidopsis* Root. *Mol Plant* 12: 648-660**

Google Scholar: [Author Only](#) [Title Only](#) [Author and Title](#)

**Zhao M, Morohashi K, Hatlestad G, Grotewold E, Lloyd A (2008) The TTG1-bHLH-MYB complex controls trichome cell fate and patterning through direct targeting of regulatory loci. *Development* 135: 1991-1999**

Google Scholar: [Author Only](#) [Title Only](#) [Author and Title](#)

**Zhou Y, Zhou B, Pache L, Chang M, Khodabakhshi AH, Tanaseichuk O, Benner C, Chanda SK (2019) Metascape provides a biologist-oriented resource for the analysis of systems-level datasets. *Nat Commun* 10: 1523**

Google Scholar: [Author Only](#) [Title Only](#) [Author and Title](#)

**Zhu HF, Fitzsimmons K, Khandelwal A, Kranz RG (2009) CPC, a single-repeat R3 MYB, is a negative regulator of anthocyanin biosynthesis in *Arabidopsis*. *Mol Plant* 2: 790-802**

Google Scholar: [Author Only](#) [Title Only](#) [Author and Title](#)